The Plant Cell, Vol. 21: 2253–2268, August 2009, www.plantcell.org

Abscisic Acid Represses Growth of the *Arabidopsis* Embryonic Axis after Germination by Enhancing Auxin Signaling [W]

Christophe Belin,[a] Christian Megies,[a] Eva Hauserová,[b,c] and Luis Lopez-Molina[a,1]

[a] Département de Biologie Végétale, Université de Genève, 1211 Genève 4, Switzerland
[b] Laboratory of Growth Regulators, Faculty of Science, Palacky University, CZ-78371 Olomouc, Czech Republic
[c] Swedish University of Agricultural Science, Umea Plant Science Center, Department of Forest Genetics and Plant Physiology, Umea 901 83, Sweden

Under unfavorable environmental conditions, the stress phytohormone ABA inhibits the developmental transition from an embryo in a dry seed into a young seedling. We developed a genetic screen to isolate *Arabidopsis thaliana* mutants whose early seedling development is resistant to ABA. Here, we report the identification of a recessive mutation in *AUXIN RESISTANT1* (*AUX1*), encoding a cellular auxin influx carrier. Although auxin is a major morphogenesis hormone in plants, little is known about ABA–auxin interactions during early seedling growth. We show that *aux1* and *pin2* mutants are insensitive to ABA-dependent repression of embryonic axis (hypocotyl and radicle) elongation. Genetic and physiological experiments show that this involves auxin transport to the embryonic axis elongation zone, where ABA enhances the activity of an auxin-responsive promoter. We propose that ABA represses embryonic axis elongation by potentiating auxin signaling in its elongation zone. This involves repression of the AUXIN INDUCIBLE (Aux/IAA) gene *AXR2/IAA7*, encoding a key component of ABA- and auxin-dependent responses during postgerminative growth.

INTRODUCTION

Early seedling development is a delicate phase in the plant life cycle during which the highly protected embryonic state in the mature seed is abandoned in favor of the fragile and autotrophic seedling state. In after-ripened (i.e., nondormant) *Arabidopsis thaliana* seeds, imbibition by water is sufficient to trigger germination. It initiates a series of visible developmental events, first that of testa rupture followed by concomitant endosperm rupture and radicle protrusion (completion of seed germination per se; Müller et al., 2006; reviewed in Bewley, 1997; Kucera et al., 2005; Holdsworth et al., 2008), further embryonic axis elongation, and finally cotyledon expansion and greening, referred to as early seedling growth distinct from germination (Müller et al., 2006; reviewed in Finch-Savage and Leubner-Metzger, 2006). Under normal conditions, these steps are completed within 48 h after seed imbibition and they do not take place without de novo biosynthesis of the phytohormone gibberellic acid (GA) (reviewed in Debeaujon and Koornneef, 2000; Finch-Savage and Leubner-Metzger, 2006). Moreover, upon seed imbibition, a drastic downregulation of embryogenesis gene expression is observed, such as that of transcription factors *ABA-insensitive3* (*ABI3*) and *ABI5* as well as that of osmotolerance genes (Parcy et al., 1994; Lopez-Molina et al., 2001; Lopez-Molina et al., 2002). However, within the first 2 d upon imbibition, a sudden osmotic stress or exposure to the stress hormone abscisic acid (ABA) can delay or block any of the developmental transition steps described above (Lopez-Molina et al., 2001). Growth arrest is also associated with reinduction of *ABI3* and *ABI5* expression, which confers osmotolerance to the embryo. Here, we investigate seed germination and postgermination growth (i.e., the steps prior to and after endosperm rupture, respectively). This study focuses on ABA-dependent repression of embryonic axis elongation, which begins prior to endosperm rupture and continues thereafter. Below, embryonic axis refers to the mature embryonic axis present in dry seeds, and embryonic axis elongation refers to the elongation of the mature embryonic axis that occurs after seed germination (i.e., after endosperm rupture).

The key roles played by GA and ABA in seed germination and early seedling development have long been established (reviewed in Olszewski et al., 2002; Nambara and Marion-Poll, 2005), and the coordination of GA- and ABA-dependent signals is starting to be unveiled (Piskurewicz et al., 2008, 2009). Other phytohormones influence the seed-to-seedling transition, but how they participate is poorly understood (Clouse, 1996; Beaudoin et al., 2000; Ghassemian et al., 2000; Steber and McCourt, 2001; Riefler et al., 2006). Auxin is a key morphogenesis hormone involved in numerous developmental programs in plants, where it notably contributes to the regulation of cell elongation (reviewed in Fleming, 2006; Teale et al., 2006). During seed germination and early seedling growth, ABA severely inhibits embryonic axis elongation and cotyledon expansion, and it is therefore surprising that auxin- and ABA-dependent interactions have not been identified in this context.

Current models of auxin action emphasize the regulation of auxin transport in and out of cells and its effect on auxin signaling factors (reviewed in Fleming, 2006; Teale et al., 2006; Benjamins

[1] Address correspondence to luis.lopezmolina@unige.ch.
The author responsible for distribution of materials integral to the findings presented in this article in accordance with the policy described in the Instructions for Authors (www.plantcell.org) is: Luis Lopez-Molina (luis.lopezmolina@unige.ch).
[W] Online version contains Web-only data.
www.plantcell.org/cgi/doi/10.1105/tpc.109.067702

and Scheres, 2008). Transport involves specific auxin carriers: PIN factors are transmembrane proteins essential for auxin efflux in cells, whereas AUX1/LAX factors are 11-transmembrane domain proteins facilitating auxin influx (reviewed in Kramer and Bennett, 2006; Kerr and Bennett, 2007). Intracellular auxin stimulates the activity of auxin response factors (ARFs), which are transcription factors regulating the expression of auxin target genes. ARFs are bound to Aux/IAA negative regulators, maintaining the former in an inactive state. The binding of auxin to TIR1-related F-box proteins enhances Aux/IAA destruction via the proteasome, thus liberating ARF activity (reviewed in Quint and Gray, 2006; Teale et al., 2006).

Interactions between auxin- and ABA-dependent responses have been described mainly in roots (Brady et al., 2003; Rock and Sun, 2005). Whole-genome expression studies showed that, during seed germination, *AUX1*, *PIN2*, and *PIN7* mRNAs are up- and downregulated in response to GA and ABA, respectively (Ogawa et al., 2003; Nakabayashi et al., 2005; Penfield et al., 2006). Two independent reports using a *DR5:β-glucuronidase* (*GUS*) auxin signaling reporter suggested that auxin-dependent responses increase during embryogenesis and remain present in germinating seeds (Ni et al., 2001; Liu et al., 2007). Moreover, the study of the regulation of *ARF10* mRNA stability by *miR160* miRNA implicated *ARF10* in modulating ABA responsiveness during seed germination (Liu et al., 2007). These reports indicate that crosstalk between ABA- and auxin-dependent responses takes place during seed germination and early seedling development in which ABA-dependent repression of growth is potentiated by auxin.

In this study, we further explored ABA- and auxin-dependent responses during seed germination and postgermination growth after isolating an *aux1* mutant, affected in auxin transport, in a new genetic screen for mutants deficient in ABA responses. *aux1* was identified as a recessive locus displaying resistance to ABA during the seed-to-seedling developmental transition. We show that *AUX1* is specifically required for ABA-dependent repression of embryonic axis elongation. This process requires specific auxin transport to the peripheral elongation zone via AUX1 and PIN2, which are localized in the root cap and the elongation zone. In cells of those regions, ABA enhances auxin responses by downregulating *AXR2*/*IAA7* expression in an auxin-independent manner. Thus, *AXR2*/*IAA7* is at the juncture of an ABA and auxin crosstalk by acting as a negative regulator in both hormonal pathways.

RESULTS

Identification of *aux1* as a Previously Unknown ABA-Insensitive Locus

Previous screens to identify mutants displaying resistance to ABA during seed germination typically used high ABA concentrations (3 to 10 μM) to ensure efficient repression of seed germination and early seedling growth (Koornneef et al., 1984; Finkelstein, 1994; Lopez-Molina and Chua, 2000). This led to the identification of a relatively small number of *ABI* loci, notably the downstream ABA response factor *ABI5*, which represses endosperm rupture (Finkelstein and Lynch, 2000; Lopez-Molina and Chua, 2000). We sought to identify novel *ABI* loci in a transgenic context in which ABI5 accumulation is constitutive. This has the advantage of (1) avoiding the recovery of mutations in *ABI5* or in genes encoding positive regulators of *ABI5* expression (such as *ABI3*) and (2) lowering the ABA concentrations used in the screen (0.5 μM). The latter is possible because ABI5 overexpression delays germination and subsequent growth and thus facilitates the identification of mutants with altered responses to ABA (Lopez-Molina et al., 2001).

An *abi5-4*/*Pro35S:ABI5* transgenic line was mutagenized, which allowed us to identify mutants displaying resistance to ABA during the seed to seedling transition (see details in Methods). We focus here on a particular mutant phenotype initially called *long root* (*lrt*) (see Supplemental Figure 1A online). Sequencing analysis of the *Pro35S:ABI5* transgene and protein gel blot analysis of ABI5 protein levels showed that transgenic *ABI5* expression is not affected in *lrt* mutants (see Supplemental Figure 1B online). *lrt* seeds developed similarly to the parental line seeds under normal conditions but displayed accelerated growth in the presence of ABA (see Supplemental Figure 1A online). Interestingly, *lrt* mutants also displayed an agravitropic root phenotype.

The *lrt* locus was mapped to a 600-kb interval ~4 Mb from the bottom end of chromosome 2 (see Supplemental Figure 1C online). This interval contains *AUX1*, encoding an auxin influx facilitator with 11 transmembrane domains (Bennett et al., 1996; Marchant et al., 1999; Swarup et al., 2004; Yang et al., 2006). Given that *aux1* mutants display agravitropism, we postulated that *lrt* might be an *aux1* allele. DNA sequencing of the *AUX1* coding sequences in *lrt* revealed a G-to-A substitution in the fourth exon replacing a TRP codon with a STOP (position 196; see Supplemental Figure 1D online). Moreover, available recessive alleles of *aux1* (*aux1-7*, *aux1-22*, and *aux1-21*; see Supplemental Figure 1D online) displayed clear resistance to ABA during the seed to seedling developmental transition (Figure 1). Taken together, these data show that *lrt* is a previously undiscovered *aux1* allele, which we have renamed *aux1-301* to reflect its molecular identity. Below, we use previously reported *aux1* alleles to further describe the role of *AUX1* in the ABA-dependent repression taking place during the seed-to-seedling transition.

AUX1 Is Involved in ABA-Dependent Repression of Embryonic Axis Elongation during Early Seedling Development

ABA inhibits, albeit with different efficiencies, the completion of all the steps of seed germination and early seedling development, which chronologically involve testa rupture, endosperm rupture, embryonic axis elongation, cotyledon expansion, and greening. Testa and endosperm rupture responses to ABA were similar between wild-type and *aux1* seeds, although endosperm rupture in *aux1* appeared to be mildly resistant to ABA, suggesting that *aux1* resistance to ABA is mostly postgerminative (see Supplemental Figure 2 online). Thus, we wished to assess directly embryonic axis elongation in response to ABA by performing transfer experiments upon endosperm rupture (i.e., axis emergence out of testa and endosperm layers). This has the advantage of eliminating the mechanical constraint imposed by an unruptured endosperm layer.

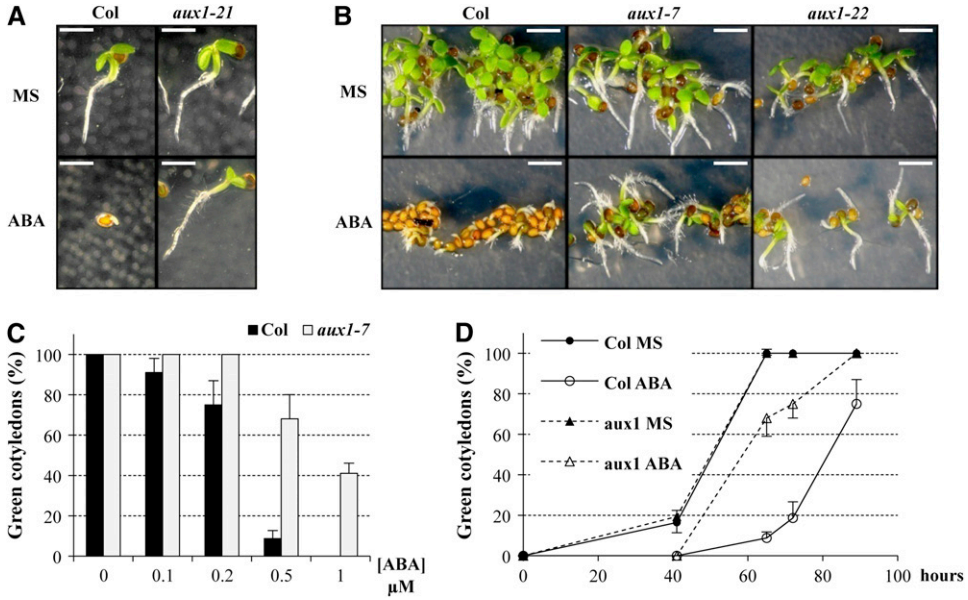

Figure 1. *aux1* Mutant Early Seedling Growth Is Resistant to ABA.

(A) The pictures show wild-type (Columbia [Col]) and *aux1-21*, 89 h after seed imbibition in the absence (Murashige and Skoog [MS]) or presence of 0.5 µM ABA (ABA). Bars = 1 mm.

(B) The pictures show wild type (Col), *aux1-7*, and *aux1-22*, 90 h after seed imbibition in the absence (MS) or presence of 0.5 µM ABA (ABA). Bars = 1 mm.

(C) Percentage of emerged green cotyledons for wild type (black bars) and *aux1-7* mutant (light-gray bars) was scored 89 h after seed imbibition in the presence of different ABA concentrations, as indicated. Means + SD are shown (n = 2).

(D) Time course of the percentage of emerged green cotyledons in wild-type (Col; plain line) and *aux1-7* (aux1; dashed line) populations after seed imbibition on medium in the absence (MS; closed symbols) or presence (ABA; open symbols) of 0.2 µM ABA. Means + SD are shown (n = 2).

In this assay, ABA markedly repressed wild-type axis elongation (Figure 2). By contrast, the elongation of *aux1-21* embryonic axis occurred in virtually the same manner in presence or absence of ABA. *aux1* mutants elongated their embryonic axis slightly faster relative to the wild type in the absence of ABA (Figure 2).

These data show that *AUX1* is necessary to repress embryonic axis elongation in response to ABA. In this context, faster axis elongation in *aux1* embryos in the absence of ABA may reflect their resistance to the endogenous ABA pools present in germinating seeds (Piskurewicz et al., 2008). We also noticed that cotyledon expansion and greening were also resistant to ABA in *aux1* embryos (Figures 1C and 1D). Since this may indirectly result from faster embryonic axis growth in *aux1* embryos on ABA, we focused our studies to the repression of embryonic axis elongation by ABA.

AUX1 Functions in the Root Cap to Mediate ABA-Dependent Responses

We used a previously described *AUX1* promoter transgenic line (WT/*ProAUX1:AUX1-YFP*; Swarup et al., 2004) to locate AUX1-yellow fluorescent protein (YFP) fusion protein during early development (Figure 3). Under normal conditions and prior to endosperm rupture (i.e., 32 h after seed imbibition), AUX1-YFP could be detected only in the plasma membrane of lateral root cap and columella cells. Thereafter, during axis elongation, AUX1-YFP fluorescence spread to the plasma membrane of epidermal cells. Upon completion of axis elongation, AUX1-YFP could be detected in the plasma membrane of the root cap, the protophloem, and all epidermal tissues of both shoots and roots, consistent with previous reports examining AUX1-YFP fluorescence in seedlings (Dharmasiri et al., 2006). AUX1-YFP fluorescence in the plasma membrane of root cap cells did not show obvious evidence of polarization (Figure 3B; see Discussion). ABA treatment blocked axis elongation and did not significantly alter the pattern of AUX1-YFP localization, which was maintained in the plasma membrane of the lateral root cap and columella cells (see Supplemental Figure 3A online).

RNA gel blot analysis showed that *AUX1* mRNA, undetected in dry seeds, could be detected 24 h after seed imbibition (i.e., before endosperm rupture) in wild-type seeds under normal imbibition conditions (see Supplemental Figure 3B online). Thereafter, *AUX1* mRNA levels increased, consistent with the observed spread of AUX1-YFP expression along the axis. *AUX1* mRNA levels remained low in presence of ABA, similar to those found 24 h after seed imbibition, consistent with the restricted AUX1-YFP localization to the lateral root cap and columella cells (see Supplemental Figure 3B online).

These data indicate that AUX1 is localized mainly in the root cap at the time of endosperm rupture and thereafter during axis elongation. Moreover, ABA appears to limit *AUX1* expression rather than altering AUX1 localization.

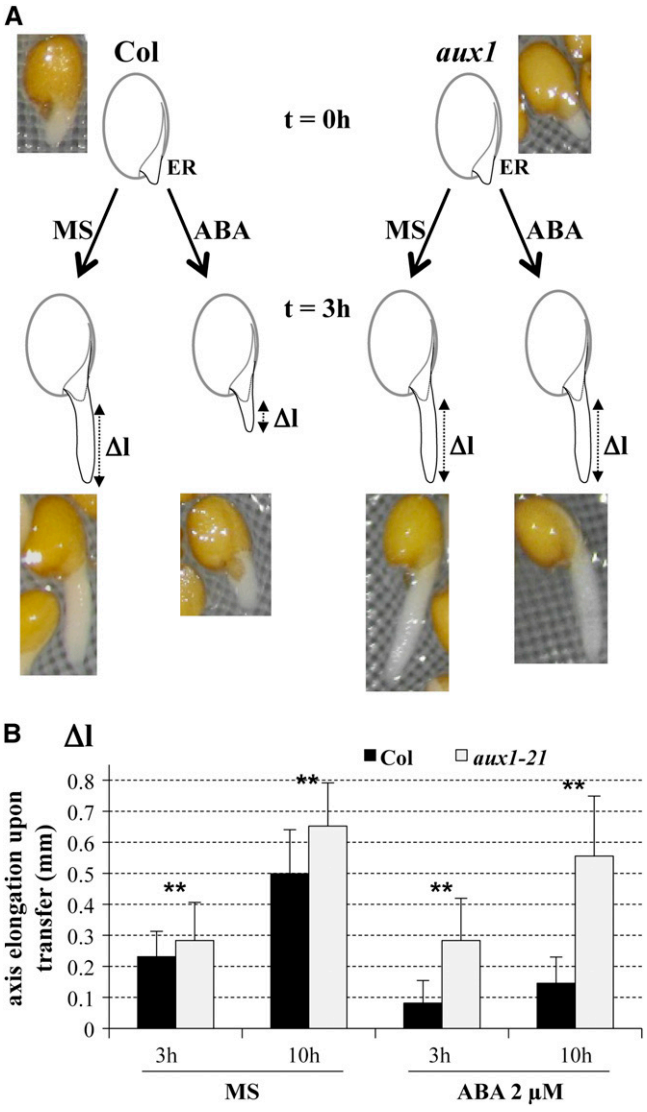

Figure 2. *aux1-21* Embryonic Axis Elongation Is Insensitive to ABA.

(A) Diagrams and representative pictures showing embryonic axis elongation (Δl) upon endosperm rupture (ER) of the wild type (Col) and *aux1-21* (*aux1*). Seeds were imbibed on normal medium (MS) and transferred at t = 0 h (time of endosperm rupture) to either MS or MS supplemented with 2 μM ABA (ABA).

(B) Elongation (Δl) quantification of the experiment described in **(A)**. This graph shows the axis elongation of Col (black bars) and *aux1-21* (light-gray bars) between t = 0 h and 3 or 10 h, as indicated, on MS or 2 μM ABA. Standard deviations are shown ($n \geq 20$). Asterisks indicate a significant difference between the wild type and the mutant, based on a two-tailed *t* test ($P < 0.01$).

Auxin- and ABA-Dependent Responses Coenhance Each Other to Repress Embryonic Axis Elongation

AUX1 was previously described as an auxin influx facilitator; therefore, we wanted to explore whether auxin is involved in the ABA-dependent repression of embryonic axis elongation.

1-Naphthoxyacetic acid (NOA), a specific inhibitor of auxin influx carriers (Parry et al., 2001), was used to characterize axis elongation in the absence or presence of ABA. Repression of embryonic axis elongation by ABA was reduced in wild-type plants in the presence of NOA (Figure 4A). By contrast, exogenous application of auxin repressed wild-type embryonic axis elongation (Figure 4B). Moreover, 1-napthalene acetic acid (NAA), a lipophilic synthetic form of auxin diffusible through cell membranes, repressed *aux1* embryonic axis elongation, but 2,4-D, which requires auxin influx carrier activity to penetrate into cells, did not, consistent with previous reports (Figure 4B;

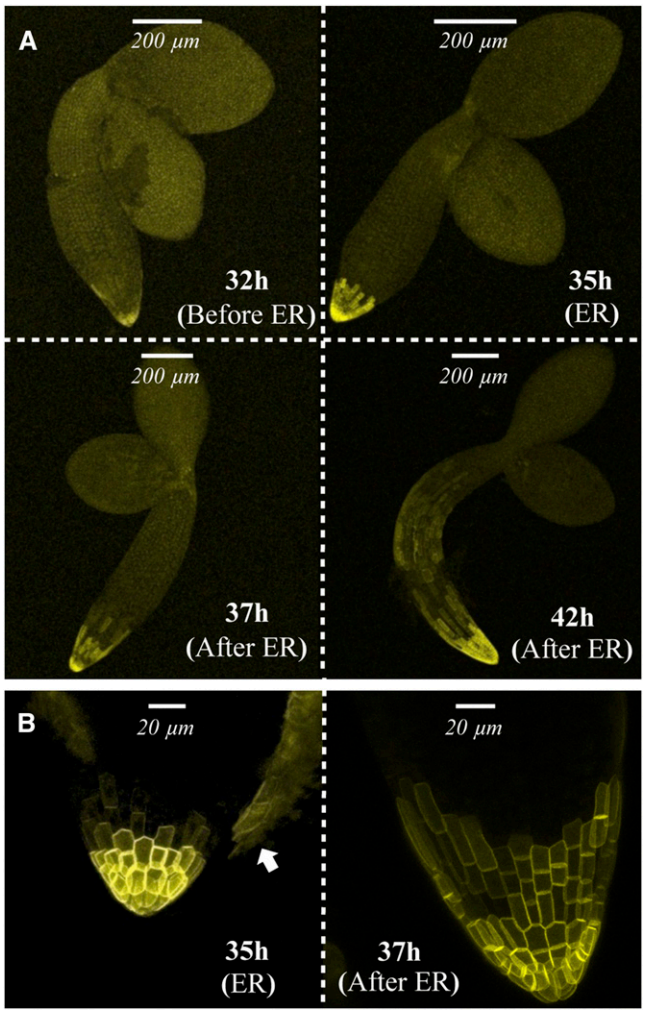

Figure 3. AUX1 Is Localized in the Plasma Membrane of Lateral Root Cap Cells and Columella Cells during Seed Germination.

Confocal microscopy imaging of an AUX1-YFP fusion expressed under the control of the endogenous *AUX1* promoter in Col background.

(A) Pictures of dissected embryos at 4 stages: 3 h prior to endosperm rupture (ER; i.e., 32 h after seed imbibition), ER (35 h after seed imbibition), and during the elongation of the embryonic axis (37 and 42 h).

(B) Magnified pictures of the lateral root cap area of intact germinating seeds at the time of ER (35 h) and during elongation of the embryonic axis (after ER). The arrow indicates testa autofluorescence.

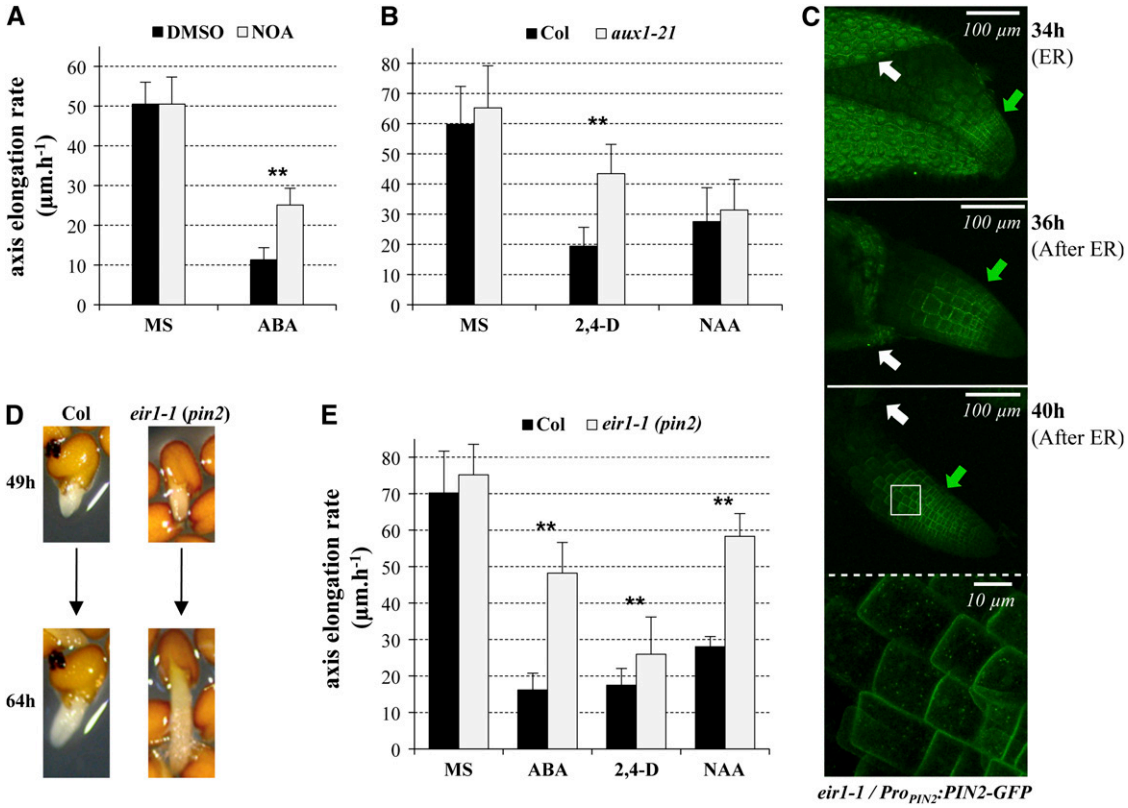

Figure 4. Auxin Transport Is Necessary to Mediate ABA-Dependent Repression of Embryonic Axis Elongation.

(A) NOA treatment inhibits ABA-dependent repression of embryonic axis elongation. Graph representing the embryonic axis elongation rate of wild type (Col), with (light gray bars) or without 2 μM NOA (dark bars), either in the absence (MS) or presence of 0.5 μM ABA in the medium.

(B) Auxin represses embryonic axis elongation. Graph representing the embryonic axis elongation rate of Col (black bars) and *aux1-21* (light-gray bars) grown on normal medium (MS) or medium supplemented with synthetic auxins 1 μM NAA or 0.5 μM 2,4-D, as indicated.

(C) PIN2 is localized in lateral root cap cells and elongating peripheral (epidermis and cortex) cells during germination. Confocal microscopy imaging of a PIN2-GFP fusion expressed under the control of the endogenous *PIN2* promoter in *eir1-1* (*pin2*) background. Whole-embryo pictures at three stages during the axis elongation after endosperm rupture (ER). The fourth picture shows a magnification of the area indicated by the square in the third picture. White arrows indicate testa autofluorescence, and green arrows indicate PIN2-GFP fluorescence.

(D) *pin2* embryonic axis elongation is insensitive to ABA. Pictures show representative wild-type (Col) and *pin2* (*eir1-1*) germinating seeds, 49 and 64 h after imbibition in presence of 0.5 μM ABA.

(E) Embryonic axis elongation rates in Col (black bars) and *eir1-1* (light-gray bars) plants grown on normal medium (MS) or medium supplemented with 0.5 μM ABA, 1 μM NAA, or 0.5 μM 2,4-D, as indicated.

For **(A)**, **(B)**, and **(E)**, the *y* axis represents the average embryonic axis elongation rate ($\mu m \cdot h^{-1}$). Standard deviations are indicated ($n \geq 15$). Asterisks indicate a significant difference between the wild type and the mutant, based on a two-tailed *t* test ($P < 0.01$).

Marchant et al., 1999). Taken together, these observations are consistent with the notion that auxin represses embryonic axis elongation during early seedling growth.

PIN factors are required for cellular auxin efflux (reviewed in Kramer and Bennett, 2006). We therefore studied the role of PIN factors in repressing axis elongation in response to ABA as well as their expression and localization during early seedling development. *PIN2*, *PIN3*, *PIN4*, and *PIN7* gene expression was followed using previously described transgenic lines carrying *PIN* promoter fusions with the reporter genes *GUS* or green fluorescent protein (*GFP*).

PIN4 promoter activity could not be detected using the *ProPIN4:GUS* reporter line (see Supplemental Figure 4A online); moreover, wild-type and *pin4-3* seeds displayed similar responses to ABA during the seed-to-seedling transition (see Supplemental Figure 4B online). This suggested that *PIN4* does not play a significant role in mediating ABA responses during early seedling growth. Staining patterns obtained with *ProPIN3:GUS* and *ProPIN7:GUS* reporter lines indicated that *PIN3* and *PIN7* are both expressed in vascular tissues and the radicle tip, whereas *PIN7* is expressed specifically in the peripheral tissues of the future hypocotyl (see Supplemental Figure 4A online). However both *pin3-5* and *pin7-2* mutants displayed normal repression of embryonic axis elongation in response to ABA (see Supplemental Figure 4B online). In the case of *PIN2*, we used a *ProPIN2:PIN2-GFP* line (Xu and Scheres, 2005), which showed that PIN2-GFP protein is present in the

epidermis and cortex of the elongation zone and is also detectable in the lateral root cap cells, although to a lower extent (Figure 4C). The PIN2-GFP fusion protein was polarly localized in the upper part of the plasma membrane of embryonic axis elongating cells (Figure 4C). Strikingly, *pin2* (*eir1-1* allele) axis elongation was markedly resistant to ABA, while otherwise being similar to that of the wild type under normal conditions (Figures 4D and 4E). The *pin2* mutant was also resistant to NAA-induced repression of embryonic axis elongation but displayed a very mild insensitivity to 2,4-D, unlike *aux1* mutants (Figure 4E). This is consistent with previous reports showing that NAA, but not 2,4-D, is efficiently transported through auxin efflux transporters and that *pin2* insensitivity to NAA is much stronger than its insensitivity to 2,4-D for root growth and gravitropism in older plants (Delbarre et al., 1996; Müller et al., 1998).

Taken together, these observations strengthen the notion that auxin flows in the epidermis and cortex of the axis elongation zone are critical to repress elongation in response to ABA.

ABA Potentiates Auxin Responses without Increasing Overall Auxin Levels

We wished to distinguish whether auxin-mediated repression of axis elongation is the result of increased auxin levels or increased auxin-dependent responses.

To test whether ABA potentiates auxin signaling, we examined whether the combination of low auxin and low ABA concentrations synergistically repress axis elongation. For this purpose, we examined the effect of diffusible auxin (NAA) in an *aux1* mutant genetic background where endogenous auxin flow is presumed to be drastically diminished. Titration experiments revealed that concentrations up to 0.1 μM NAA and 0.2 μM ABA did not affect *aux1* axis elongation per se (Figures 5A and 5B). However, in combination, 0.05 μM NAA and 0.05 μM ABA markedly repressed *aux1* axis elongation (Figure 5A). These observations are consistent with the notion that ABA locally enhances auxin-dependent repression of axis elongation.

To further explore the role of auxin in ABA-dependent repression of embryonic axis growth, we monitored embryonic axis elongation in *abi* mutants in response to auxin. We reasoned that if ABA represses embryonic axis elongation solely by increasing auxin levels, then axis elongation in *abi* mutants would be as sensitive to auxin as it is in wild-type plants since, in this view, auxin acts as the final downstream parameter determining the rate of axis elongation. By contrast, if ABA potentiates auxin signaling pathways, as suggested above, one may expect auxin signaling pathways to be repressed in *abi* mutants. Thus, exogenous auxin application should induce weaker repression of embryonic axis elongation in *abi* mutants relative to wild-type plants. Consistent with this hypothesis, we indeed observed auxin (NAA and 2,4-D) insensitivity at the level of embryonic axis elongation in *abi4-1* and *abi5-3* mutants (Figure 5C). No striking insensitivity was observed in the weak *abi3-9* allele (Nambara et al., 2002).

To further characterize the interaction between auxin- and ABA-dependent signals, we used a WT/*ProIAA2:GUS* line carrying the promoter sequence of the auxin-responsive gene *IAA2* fused to the GUS reporter (Swarup et al., 2001).

GUS staining of a WT/*ProIAA2:GUS* line showed that the *IAA2* promoter is active mainly in the vascular tissues and lateral root

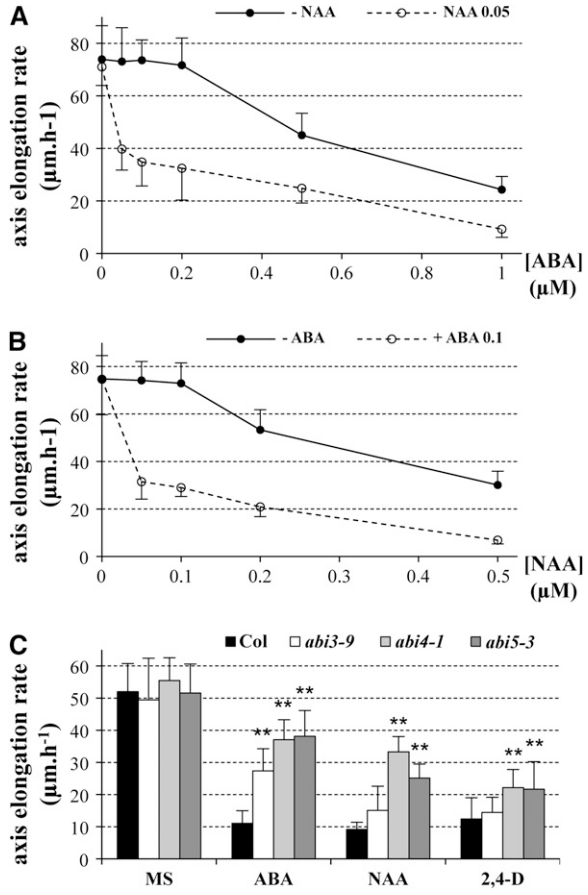

Figure 5. ABA Potentiates the Effect of Diffusible Auxin NAA to Repress Embryonic Axis Elongation.

(A) Average embryonic axis elongation rate of *aux1-21* grown on normal medium (-NAA, plain line) or medium supplemented with diffusible synthetic auxin 0.05 μM NAA (NAA 0.05, dashed line), in the presence of different concentrations of ABA.

(B) Average embryonic axis elongation rate of *aux1-21* grown on normal medium (-ABA, plain line) or medium supplemented with 0.1 μM ABA (+ABA 0.1, dashed line) in the presence of different concentrations of the synthetic auxin NAA.

(C) Average embryonic axis elongation rate of wild type (Col, black bars), *abi3-9* (white bars), *abi4-1* (light-gray bars), and *abi5-3* (dark-gray bars) grown on normal medium (MS) or medium supplemented with 0.5 μM ABA, 0.5 μM 2,4-D, or 1 μM NAA, as indicated. Asterisks indicate a significant difference between the wild type and the mutant, based on a two-tailed *t* test ($P < 0.01$).

For **(A)** to **(C)**, standard deviations are represented ($n \geq 15$).

cap during embryonic axis elongation under normal conditions (Figure 6A). By contrast, blue staining showed that *IAA2* promoter activity was strongly activated in peripheral tissues (epidermis and/or cortex) of the elongation zone upon transfer to ABA, which also efficiently repressed embryonic axis elongation (Figure 6A). By contrast, no blue staining could be detected in the epidermis or cortex in response to ABA in an *aux1* genetic background (*aux1*/*ProIAA2:GUS* reporter line) where it could be detected only in the vascular tissues and the radicle tip

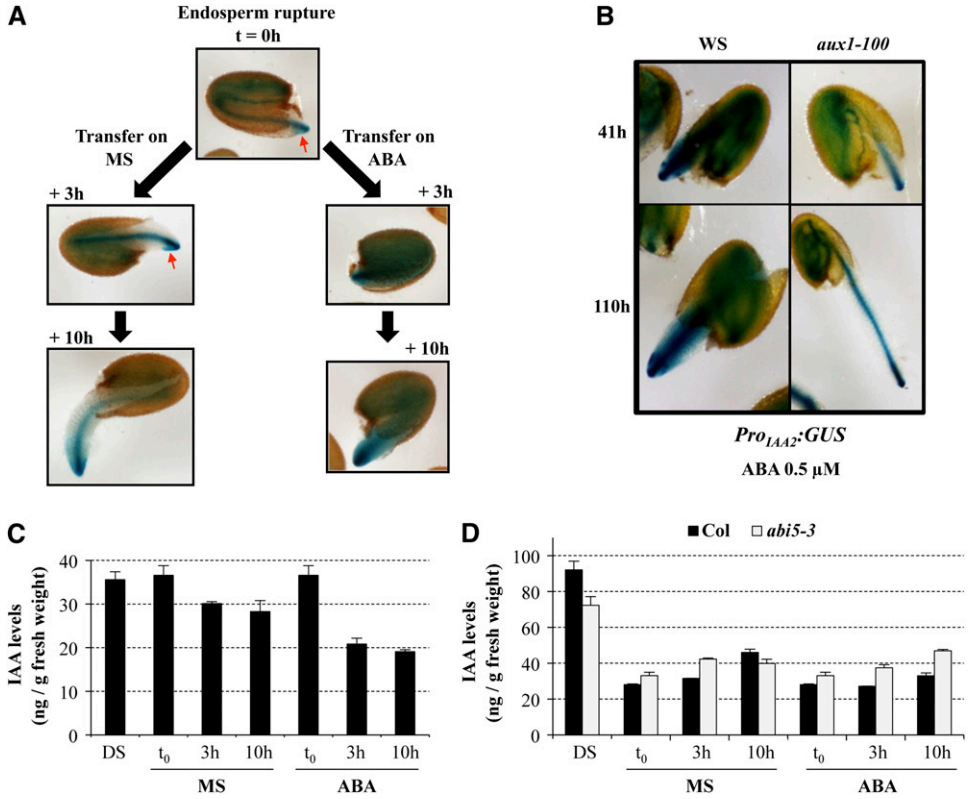

Figure 6. ABA Potentiates Auxin Responses in the Elongation Zone Rather Than Increasing Auxin Levels.

(A) Activation of the *IAA2* promoter in the elongating zone after endosperm rupture (ER) in response to ABA. Wild-type (Wassilewskija [WS]) lines expressing the *uidA* gene under the control of the *IAA2* promoter were transferred upon ER to normal medium (MS, left panels) or medium supplemented with 2 µM ABA (right panels). Whole seed staining was performed just prior transfer (t = 0 h) and 3 or 10 h thereafter. Red arrows indicate the asymmetric distribution of staining resulting from gravitropic response.

(B) ABA-dependent stimulation of transgenic *IAA2* promoter requires *AUX1*. Wild-type (WS) or *aux1* (*aux1-100*) seeds expressing the *uidA* gene under the control of the *IAA2* promoter were sown on medium with 0.5 µM ABA. Whole-seed staining was performed 41 and 110 h after imbibition for each genotype.

(C) Global auxin levels in early seedlings in response to ABA. Auxin levels were measured in the same samples used in **(A)** and in dry seeds (DS).

(D) Auxin levels in Col and *abi5-3* early seedlings, transferred upon endosperm rupture (ER) to normal medium (MS) or medium supplemented with 2 µM ABA. Auxin levels were measured as in **(C)** just prior to transfer (t_0) and 3 or 10 h thereafter. Auxin levels in dry seeds (DS) are also shown.

In **(C)** and **(D)**, means + SD are shown (n = 3).

irrespective of the presence or absence of ABA (Figure 6B). Taken together, these data strongly suggest that ABA-dependent activation of the *IAA2* promoter in peripheral tissues of the elongation zone involves auxin signals that are elicited in response to ABA. They also indicate that activation of *IAA2* expression by ABA requires auxin transport through AUX1.

Stimulation of *ProIAA2:GUS* activity in response to ABA (Figure 6A) could be due to an increase of auxin synthesis, an activation of auxin signaling, or both. We measured auxin levels (see Methods) in whole embryos of *ProIAA2:GUS* reporter lines upon endosperm rupture and thereafter, after transfer to a medium with or without ABA (2 µM). Indole-3-acetic acid (IAA) levels were similar between dry seeds and seeds harvested 36 h after their imbibition (i.e., at the time of endosperm rupture). Thereafter, embryonic axis elongation ensued and IAA levels slowly decreased in the absence of ABA (measured 3 and 10 h after endosperm rupture [t = 0 h]; Figure 6C). The presence of ABA upon transfer did not prevent the decrease in IAA levels (Figure 6C), although it prevented embryonic axis elongation, and further development was arrested or strongly delayed (Figure 6A). The absence of *ABI5* (as in *abi5-3* mutants) did not appear to alter auxin levels markedly relative to the wild type (Figure 6D). The data further support the notion that auxin levels decay upon wild-type seed imbibition irrespective of the absence or the presence of ABA (Figure 6D).

Taken together, these observations support the view that ABA potentiates auxin signaling rather than altering auxin levels to repress embryonic axis elongation.

AXR2/*IAA7* and *AXR3*/*IAA17* Inhibit ABA- and Auxin-Dependent Repression of Embryonic Axis Growth

We sought to identify auxin signaling components mediating ABA-dependent repression of embryonic axis elongation. In the current view of auxin signaling, auxin promotes degradation of

Aux/IAA negative regulators through binding to TIR1-related F-box proteins, which in turns frees ARFs that regulate the expression of auxin-responsive genes (reviewed in Quint and Gray, 2006; Teale et al., 2006). Hence, we investigated responses to ABA during the seed-to-seedling transition of mutants affected in *TIR1*, *TIR1*-related (*AFB*), *Aux/IAA*, and *ARF* genes (see Supplemental Table 1 online).

All the mutants affected in *TIR1* and *TIR1*-related F-box genes (*tir1-1*, *afb1-1*, *afb2-1*, and *afb3-1*) displayed normal repression of embryonic axis elongation in response to ABA. Similarly, mutant seeds for the more distantly related F-box genes *AFB4* and *AFB5* did not display large alterations in their ABA responses. Normal responses in single F-box mutations could be due to F-box gene redundancy in ABA-dependent repression of embryonic axis elongation, or, alternatively, other F-box proteins could be implicated. We were unable to explore responses to ABA in multiple mutant combinations of *tir1-1* and other *afb* mutant alleles (*afb1-1*, *afb2-1*, and *afb3-1*) because they are present in different ecotypes, which naturally display different responses to ABA during the seed to seedling transition.

To explore further the role of TIR1/AFB F-box proteins in the ABA-mediated repression of embryonic axis elongation, we examined the effect of two anti-auxin probes on ABA sensitivity. These synthetic auxin antagonists were obtained by adding different chains to the α-position of IAA. BH-IAA [α-(*tert*-butoxycarbonylaminohexyl)-IAA] was previously reported as the most efficient anti-auxin compound among a series of α-alkyl derivatives (Hayashi et al., 2008b), whereas PEO-IAA [α-(phenyl ethyl-2-one)-IAA] is a new compound, displaying an even more efficient anti-auxin activity (Hayashi et al., 2008a). The IAA moiety of BH-IAA has been shown to be located in the auxin binding pocket of TIR1 in the same way as natural IAA, whereas the alkyl chain is directed in the Aux/IAA binding cavity, thus preventing access of the domain II Aux/IAA degron to this cavity (Hayashi et al., 2008b). The results shown in Figure 7A show that BH-IAA and PEO-IAA are able to reduce the sensitivity of embryonic axis elongation to ABA. Indeed, ABA decreases the elongation rate of the embryonic axis by almost 80% in the absence of auxin antagonists, whereas it decreases the elongation rate only by 60 and 55% in the presence of 50 μM BH-IAA and PEO-IAA, respectively ($P < 0.01$). These results are consistent with the notion that the Aux/IAA degradation mediated by TIR1/AFB F-box proteins participates in the ABA- and auxin-dependent repression of embryonic axis elongation.

We also analyzed the early seedling growth responses to ABA of available insertion lines in all *ARF* genes as well as in previously characterized *arf* mutants (see Supplemental Table 1 online). None of these mutants exhibited altered responses to ABA during embryonic axis elongation. As above, this could suggest redundancy between members of this family, consistent with what is generally observed for *ARF* genes in other auxin-dependent responses (Wang et al., 2005; Weijers et al., 2005; reviewed in Guilfoyle and Hagen, 2007).

We next investigated early seedling growth responses to ABA in single mutants for *Aux/IAA* genes (see Supplemental Table 1 online), focusing in particular on those expressed during germination and that appear to be regulated by ABA (*IAA16*, *IAA20*, *IAA26*, *IAA28*, and *IAA29*) according to whole-genome gene expression profiling databases (Winter et al., 2007). All insertion lines in these genes exhibited normal embryonic axis growth sensitivity to ABA. Since normal responses in single *Aux/IAA* genes insertion lines could again reflect redundancy, we used dominant mutations in *Aux/IAA* genes, previously reported to exhibit altered hormonal responses in adult plants. *axr2-1* and *axr3-1* mutants carry point mutations preventing the degradation in response to auxin of IAA7 and IAA17, respectively, thus blocking auxin-dependent responses (Wilson et al., 1990; Timpte et al., 1994; Rouse et al., 1998; Nagpal et al., 2000). Strikingly, *axr2-1* and *axr3-1* exhibited strong insensitivity to ABA for embryonic axis elongation (Figures 7B and 7C). Moreover, axis elongation in *axr2-1* and *axr3-1* embryos was slightly faster relative to the wild type in the absence of ABA also. We next analyzed two independent recessive loss-of-function *axr2/iaa7* mutants. Strikingly, both *axr2/iaa7* recessive alleles displayed hypersensitive repression of embryonic axis elongation in response to ABA (Figures 7B and 7D).

These observations indicate that *AXR2/IAA7* (and possibly *AXR3/IAA17*) acts as a negative regulator in ABA signaling during repression of embryonic axis elongation. They also further substantiate the notion that ABA represses axis elongation by potentiating auxin signaling. Faster *axr2-1* and *axr3-1* mutant axis elongation under normal conditions may also reflect insensitive responses to endogenous ABA pools.

ABA Represses *AXR2/IAA7* and *AXR3/IAA17* Transcript Levels during Embryonic Axis Growth

Given the key role played by *AXR2/IAA7*, and possibly *AXR3/IAA17*, in ABA-dependent repression of embryonic axis growth, we examined their expression patterns during early seedling growth. Previous reports have shown that *AXR2/IAA7* and *AXR3/IAA17* expression in young seedlings is localized to the root, including its elongation zone (Tian et al., 2002; Knox et al., 2003; Muto et al., 2007; Tanimoto et al., 2007). We used *ProAXR2/IAA7:GUS* and *ProAXR3/IAA17:GUS* transgenic lines to monitor *AXR2/IAA7* and *AXR3/IAA17* promoter activity at the time of early axis elongation (Tian et al., 2002; Tanimoto et al., 2007). Strikingly, in the absence of ABA, blue staining in the embryo was restricted to the peripheral elongation zone (Figures 8A and 8B): (1) for *AXR3/IAA17*, a signal was detected during axis elongation (Figure 8B); (2) for *AXR2/IAA7*, the earliest time point of detection coincided with the emergence of the first root hairs (a developmental marker for the initiation of the root, collet, and hypocotyl) but prior to cotyledon expansion and greening (Figure 8A). No signal could be detected on ABA-arrested embryos and seedlings (see Supplemental Figure 5 online). These results are consistent with the notion that ABA represses embryonic axis elongation by stimulating auxin signaling in the peripheral cells of the elongation zone through ABA-dependent repression of *AXR2/IAA7* and perhaps *AXR3/IAA17* expression.

To unveil the effect of ABA on *AXR2/IAA7* and *AXR3/IAA17* expression, we performed a time course of *AXR2/IAA7* and *AXR3/IAA17* mRNA expression during embryonic axis elongation, in the absence or presence of ABA. RNA gel blot analysis showed that *AXR2/IAA7* and *AXR3/IAA17* mRNA expression could be detected at the time of endosperm rupture in the

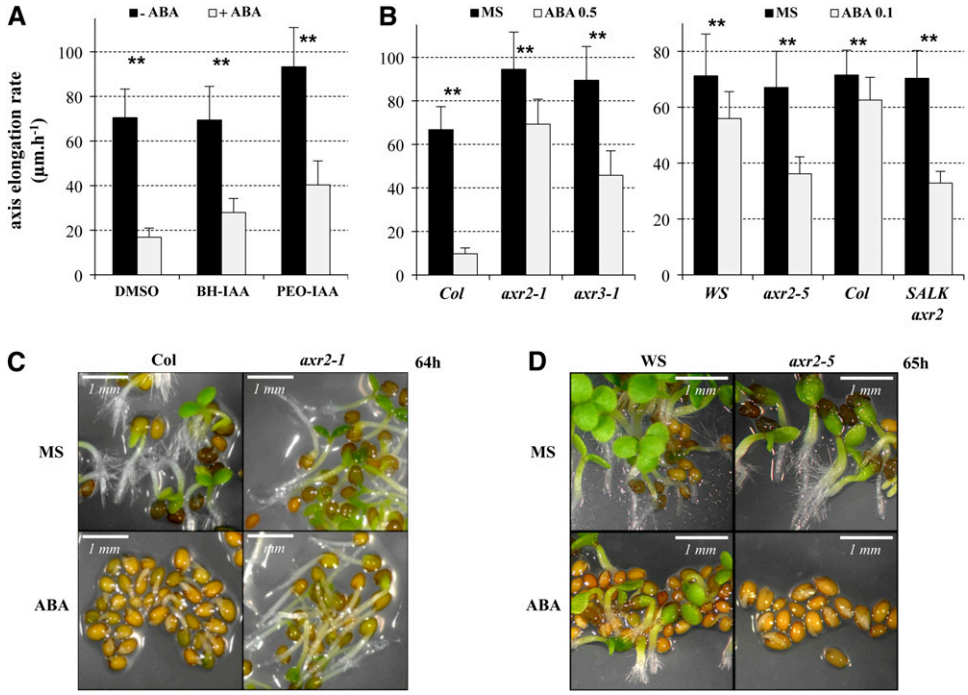

Figure 7. Aux/IAA Turnover Is Involved in ABA-Dependent Repression of Embryonic Axis Elongation.

(A) Average embryonic axis elongation rate of wild type (Col) in absence (DMSO) or presence of auxin antagonists (BH-IAA and PEO-IAA, 50 μM each) competing with endogenous IAA to bind TIR1/AFB F-box proteins. Seeds were imbibed on normal medium (MS) and transferred to different media, as indicated, either in the absence (- ABA, black bars) or presence of 2 μM ABA (+ ABA, light-gray bars).

(B) Quantification of embryonic axis elongation in *axr2/iaa7* and *axr3/iaa17* mutants. Left: average axis elongation rate of wild type (Col), *axr2-1*, and *axr3-1*, as indicated, in absence (MS, black bars) or presence of 0.5 μM ABA (light-gray bars). Right: average axis elongation rate of wild type (Col and WS), *axr2-5* (in WS ecotype), and SALK *axr2/iaa7* line (in Col ecotype), as indicated, in the absence (MS, black bars) or presence of 0.1 μM ABA (light-gray bars).

(A) And **(B)** Standard deviations are indicated ($n \geq 13$). Asterisks indicate a significant difference between untreated (-ABA or MS) and ABA-treated (+ABA or ABA) conditions, based on a two-tailed *t* test ($P < 0.01$).

(C) Pictures of seeds from wild type (Col) and *axr2-1* 64 h after imbibition in the absence (MS) or presence of 0.5 μM ABA.

(D) Pictures of seeds from wild type (WS) and *axr2-5* 65 h after imbibition in the absence (MS) or presence of 0.5 μM ABA.

absence of ABA, increasing markedly thereafter (Figure 8C). By contrast, *AXR2/IAA7* and *AXR3/IAA17* mRNA expression did not increase in the presence of ABA and remained low at all time points examined (Figure 8C). This ABA-dependent repression of *AXR2/IAA7* and *AXR3/IAA17* mRNA expression could also be observed in *aux1* mutants. Therefore, the combination of RNA gel blot analysis and promoter activity studies of both *AXR2/IAA7* and *AXR3/IAA17* suggests that the expression of *AXR2/IAA7* and *AXR3/IAA17* might be repressed by ABA in the epidermis of the elongation zone during embryonic axis growth.

Taken together, these observations support the model that ABA represses embryonic axis elongation by enhancing auxin signaling in the peripheral cells of the elongation zone through the repression of *AXR2/IAA7* and *AXR3/IAA17* expression (see model in Figure 9).

DISCUSSION

How the osmotic stress hormone ABA represses most of the complex developmental steps unfolding during the seed-to-seedling transition is incompletely understood. We unveiled the role of *AUX1*, encoding a cellular influx carrier of auxin, in the ABA-dependent inhibition of embryonic axis elongation during early seedling development. *AUX1* was identified after the positional cloning of *aux1-301/lrt*, a recessive *Arabidopsis* locus in chromosome 2, that we isolated in a genetic screen to identify *Arabidopsis* mutants with altered early seedling growth responses to ABA. So far, few mutant loci have been identified that confer resistance to ABA during seed germination and early seedling development. The identification of the *aux1-301* mutant validates the use of *abi5-4/Pro35S:ABI5* transgenic lines in genetic screens. We show that inhibition of embryonic axis elongation in response to ABA involves (1) basipetal auxin transport from the root apex to the elongation zone via AUX1 and PIN2 carriers and (2) ABA-dependent potentiation of auxin signaling responses, which could involve downregulation of the expression of the Aux/IAA genes *AXR2/IAA7* and *AXR3/IAA17* in the epidermal elongating zone of the embryonic axis. Thus, *AXR2/IAA7*, and possibly also *AXR3/IAA17*, is a negative regulator in both auxin and ABA signaling to repress axis elongation. The model shown in Figure 9 summarizes these findings and

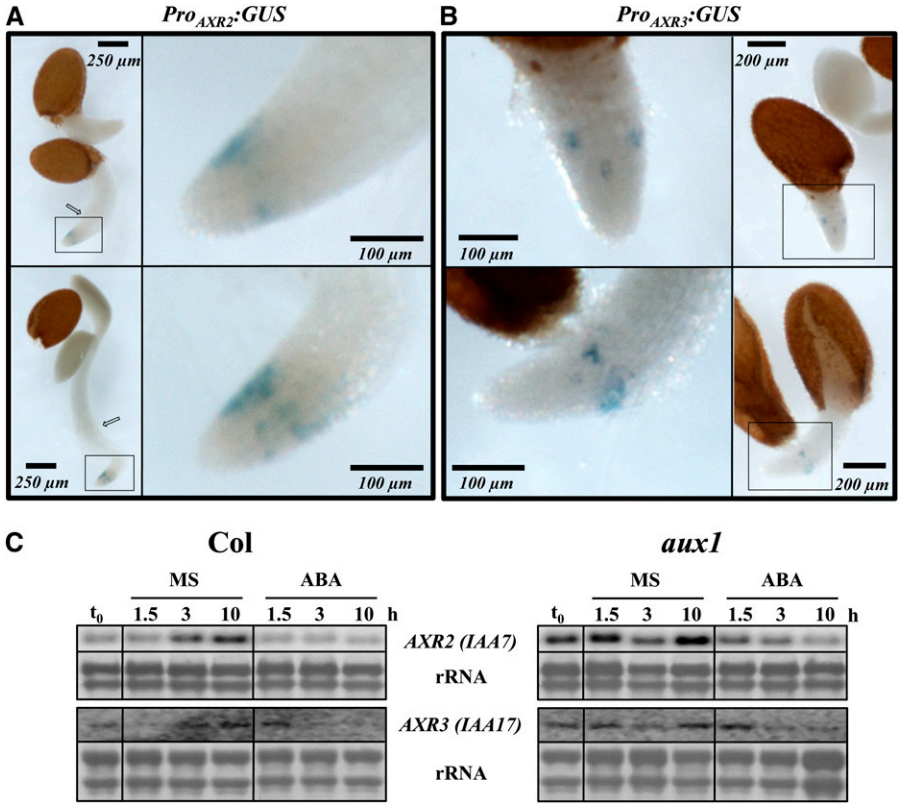

Figure 8. *AXR2/IAA7* and *AXR3/IAA17* Upstream Sequences Are Transcriptionally Active in the Peripheral Elongation Zone; ABA Represses *AXR2/IAA7* and *AXR3/IAA17* mRNA Expression.

(A) Localization of *AXR2/IAA7* promoter activity during early seedling growth. Pictures of wild-type transgenic lines expressing the *uidA* gene under the control of the *AXR2/IAA7* promoter. Whole-seed staining is visible only 42 to 45 h after seed imbibition on normal germination medium. Squares represent the areas magnified in the right panels. Arrows indicate the hypocotyl/root junction (collet).

(B) Localization of *AXR3/IAA17* promoter activity during early seedling growth. Pictures of wild-type transgenic line expressing the *uidA* gene under the control of the *AXR3/IAA17* promoter. Whole-seed staining was performed 37 h after seed imbibition on normal germination medium. Squares represent the areas magnified in the left panels.

(C) RNA gel blot analysis of *AXR2/IAA7* and *AXR3/IAA17* mRNA levels in wild-type (Col) and *aux1-21* (*aux1*) during embryonic axis elongation. Seeds were transferred upon endosperm rupture (t_0; i.e., 34 h after seed imbibition) to normal medium (MS) or medium supplemented with 2 µM ABA for 1.5, 3, or 10 h, as indicated. rRNA is shown as a loading control.

integrates the well-documented view that degradation of Aux/IAA proteins releases the activity of specific ARF factors.

In mature *Arabidopsis* embryos, the embryonic axis is a precisely patterned organ composed of hypocotyl and root precursor cells whose fate was set during embryogenesis (Scheres et al., 1994; reviewed in Jenik et al., 2007; Nawy et al., 2008) and that express specific molecular markers (e.g., *PIN7* in Supplemental Figure 4A online; Lin and Schiefelbein, 2001) . Embryonic axis differentiation toward a mature hypocotyl and root is poorly understood. At early stages of seed germination, axis precursor cells are morphologically indistinguishable, and the emergence of root hairs at the root-hypocotyl junction (the collet, see arrows in Figure 8; see Supplemental Figure 5 online) marks the first signs of differentiation, 4 to 6 h after endosperm rupture under normal conditions. This process is accompanied by hypocotyl cell elongation and greening, as well as root cell elongation and division.

During its early stages of differentiation, the axis behaves as a single organ; both hypocotyl and radicle precursor cells stop their elongation in response to ABA. At later stages (i.e., once the collet starts to differentiate), the growth inhibitory effect of ABA diminishes dramatically. We previously proposed that this early time window of responsiveness to ABA serves a physiological role: that of retaining the highly protected embryonic character of the plant before it develops into a young seedling (Lopez-Molina et al., 2001). Here, we could show that exogenous application of auxin also elicits differential responses depending on the growth stage of the axis: (1) prior to collet differentiation, auxin represses the elongation of the entire embryonic axis; (2) thereafter, auxin generally efficiently inhibits root cell elongation while it has little effect on that of hypocotyl cells, even stimulating it under certain conditions (Romano et al., 1995; Smalle et al., 1997; Gray et al., 1998; Collett et al., 2000). These observations are consistent with the existence of an early crosstalk between ABA- and

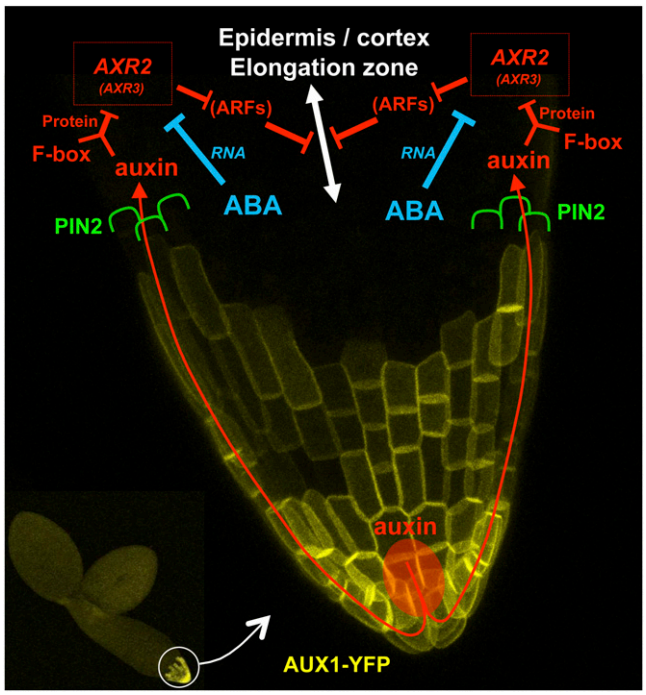

Figure 9. A Model of ABA and Auxin Crosstalk for the Repression of Embryonic Axis Elongation.

This model is drawn on a magnified confocal micrograph of the embryonic axis tip of a wild-type line expressing *ProAUX1:AUX1-YFP* (Figure 4; see Methods). Auxin (red) is distributed from the radicle tip to the elongation zone via the influx facilitator AUX1 located in the root cap (yellow) and the efflux carrier PIN2 polarly localized in the elongating epidermal and cortical cells (green). In the elongation zone, auxin activates its signaling pathway (red) by binding to TIR1/AFB F-box proteins, promoting the degradation of the Aux/IAA repressors AXR2/IAA7 and possibly AXR3/IAA17. This would, in turn, activate unknown transcriptional regulator ARFs to repress cell elongation. ARFs appear in brackets because their involvement in ABA- and auxin-dependent repression of embryonic axis elongation remains speculative. We propose that ABA (blue) potentiates the auxin pathway by strongly decreasing the mRNA levels of the Aux/IAA repressor *AXR2/IAA7* (and possibly *AXR3/IAA17*).

auxin-dependent signals to repress early axis elongation and maintain its embryonic character.

We propose that axis elongation repression in response to ABA is sustained by a basipetal auxin flow from the radicle tip toward the elongation zone via the lateral root cap. This conclusion is based on the observations that (1) AUX1 is mainly localized in the lateral root cap and columella cells (Figure 3; see Supplemental Figure 3A online); (2) PIN2 is localized to the epidermal and cortical cells of the axis elongation zone (Figure 4C); and (3) axis elongation in both *aux1* and *pin2* mutants is insensitive to ABA. In seedlings, AUX1 is polarly localized to the plasma membrane of all cell types with the notable exception of the lateral root cap and columella cells (Dharmasiri et al., 2006). Our confocal studies cannot exclude that an undetected (e.g., in internal parts of the embryo) and polarly localized AUX1 may mediate ABA-dependent repression of axis elongation. However, genetic studies have shown that AUX1 polar distribution absolutely requires *AXR4*, which encodes a protein of unknown function (Dharmasiri et al., 2006). We noticed that *axr4-2* recessive mutants have normal early seedling growth responses to ABA (see Supplemental Figure 6 online). This may be taken as an indirect indication that no undetected and polarly localized AUX1 plays any large role in repressing axis elongation in response to ABA.

We provided evidence that ABA enhances auxin-dependent signaling rather than increasing auxin flow or auxin levels, and we identified *AXR2/IAA7* as a central component of both ABA- and auxin-dependent pathways. This is based on the observations that (1) axis growth in *axr2-1* mutants, bearing a dominant mutant form of *AXR2/IAA7* preventing ARF factor activity, is strongly insensitive to ABA, whereas (2) axis growth in the recessive, loss-of-function, *axr2/iaa7* mutant alleles is hypersensitive to ABA.

In addition to *Aux/IAAs*, auxin is known to induce the expression of other auxin-responsive gene families, such as *GH3* (for *GRETCHENHAGEN-3*) and *SAUR* (for *Small Auxin Up-Regulated*) genes. To better document the general effect of ABA on auxin-responsive genes, we investigated the expression of *GH3.5*, *GH3.6*, *SAUR9*, and *IAA2* mRNA in whole embryos at the time of embryonic axis elongation. RNA gel blot analysis indicates the occurrence of a moderate and transient increase in *GH3.5*, *GH3.6*, and *SAUR9* mRNA expression 1.5 to 3 h upon transfer to ABA after endosperm rupture (see Supplemental Figure 7 online). However, thereafter, ABA tends overall to restrain auxin-responsive gene expression such that *GH3.5*, *GH3.6*, *SAUR9*, and *IAA2* mRNA expression remains at the similar low levels found prior to transfer (note that in the case of *SAUR9*, the blot is overloaded at 10 h). By contrast, *GH3.5*, *GH3.6*, *SAUR9*, and *IAA2* mRNA expression increased 10 h after transfer under normal conditions (i.e., after completion of embryonic axis elongation). Overall, our data could be compatible with the notion that ABA triggers a rapid increase in auxin signaling that may or may not occur at the whole embryo level. However, thereafter, it appears that ABA limits the expression of auxin-responsive genes over time at the whole embryo level. This may be the consequence of the ABA-dependent arrest of development (perhaps associated with auxin levels permanently kept low; Figures 6C and 6D) rather than a reflection of increased auxin signaling in the elongation zone, which involves a restricted number of cells. Indeed, the auxin-responsive genes analyzed here are not necessarily expected to be solely expressed in the elongation zone as it is clearly apparent for *IAA2* (Figures 6A and 6B).

The pattern of *AXR2/IAA7* expression during early seedling development suggests a mechanism by which ABA would enhance auxin signaling. Indeed, under normal conditions, *AXR2/IAA7* expression increases during embryonic axis elongation but is markedly repressed upon ABA treatment (Figure 8C). The fact that *AXR2/IAA7* promoter activity is detected mainly in the epidermal elongation zone during early development (Figure 8A) suggests that this ABA-dependent repression affects *AXR2/IAA7* levels in this zone. This repression appears to be specific to ABA. Indeed, on one hand auxin tends to stimulate *Aux/IAA* gene expression, including that of *AXR2/IAA7* (Abel et al., 1995). On the other hand ABA also represses *AXR2/IAA7* mRNA levels in *aux1* mutants, in which auxin flow to the elongation zone is expected to be drastically reduced (Figure 8C). Thus, ABA may

stimulate auxin signaling by directly repressing *AXR2/IAA7* mRNA expression and perhaps also that of *AXR3/IAA17*.

If *AXR2/IAA7* were to be the sole factor repressing auxin signaling in response to ABA, then in its absence (as in a *axr2/iaa7* knockout mutant), the plant would fail to respond to ABA and would not repress axis elongation (i.e., would be insensitive to ABA). Since this is not what we observe, we must speculate that *AXR2/IAA7* is not the sole *Aux/IAA* being targeted by ABA or that ABA potentiates auxin signaling in other ways or both. The view that other *Aux/IAA* factors are being targeted by ABA is consistent with our observations that (1) *AXR3/IAA17* upstream promoter sequences are actively transcribed in the elongation zone and (2) ABA represses *AXR3/IAA17* mRNA levels (Figure 8C).

Downregulation of *AXR2/IAA7* mRNA levels by ABA could involve transcriptional repression by transcription factors ABI3 and ABI5, whose role as positive regulators of ABA signaling during seed germination and early seedling growth is well established (Lopez-Molina et al., 2002). ABI5 belongs to a family of basic leucine-zipper transcription factors binding to ACGT-containing ABA-responsive elements (ABREs; Lopez-Molina and Chua, 2000; Carles et al., 2002). By contrast, ABI3 DNA binding activity has not been clearly established, although some authors have proposed that ABI3 may interact with ABI5 to regulate gene transcription (Finkelstein et al., 2002). Analysis of *AXR2/IAA7* and *AXR3/IAA17* promoter sequences revealed a canonical ABRE element (CACGTG) in each gene within 100 bp upstream of the transcription start site defined according to the cDNA sequences available in The Arabidopsis Information Resource database (http://www.Arabidopsis.org/). This suggests that ABI3 and ABI5 may interact to repress *AXR2/IAA7* and *AXR3/IAA17* transcription by binding to this particular ABRE element. *AXR2/IAA7* and *AXR3/IAA17* mRNA levels could also be downregulated posttranscriptionally given that a number of RNA binding proteins have been shown to modulate ABA signaling responses. For example, *ABH1*, encoding a CAP binding protein, negatively regulates ABA signaling during seed germination in an unknown manner (Hugouvieux et al., 2001). Thus, ABH1 may interfere with the capping process of *AXR2/IAA7* and *AXR3/IAA17* transcripts, leading to their destabilization.

Aux/IAA factors repress auxin responses by binding to ARF transcriptional factors, thus maintaining them in an inactive form (reviewed in Quint and Gray, 2006). ARF factors are known to act redundantly in auxin-dependent responses, and it is therefore not surprising that we could not identify a single recessive mutation in an *ARF* gene affected in ABA-dependent repression of embryonic axis growth (Wang et al., 2005; Weijers et al., 2005; reviewed in Guilfoyle and Hagen, 2007). The putative ARF factors targeted by AXR2/IAA7 remain to be identified. A previous report indicated that *ARF10* participates in repressing the seed-to-seedling transition in response to ABA. Indeed, lines overexpressing *miR160*, which targets the degradation of *ARF10*, *ARF16*, and *ARF17* mRNAs, and a line expressing *mARF10*, containing a mutated version of *ARF10* preventing its recognition by *miR160*, were reported to display hypersensitive and insensitive responses to ABA during early development, respectively (Liu et al., 2007). However, we found that these lines had normal axis growth responses to ABA under our experimental conditions. Thus, *ARF10* may be involved in ABA-dependent processes other than embryonic axis elongation, such as endosperm rupture. Interestingly, genetic analysis showed that *ARF10* and *ARF16* are necessary for root cap formation in a redundant manner (Wang et al., 2005). Together with our finding that root cap-derived basipetal auxin flow is critical for ABA-dependent repression of axis growth, the observations by Liu et al. (2007) could be explained by a severe alteration of the auxin flow in the abnormal root cap rather than a signaling defect due to the absence of ARF10.

Further studies are needed to identify the cellular processes targeted by auxin to prevent early axis elongation. Auxin has been proposed to modulate cellular elongation by regulating the activity of ion channels, which influence cell turgor, as well as the expression and product activity of genes encoding cell wall components. The latter includes genes encoding expansins (e.g., *EXPα1*), xyloglucan modifying enzymes (e.g., *XTR8*), and pectin methylesterases whose expression is regulated by auxin and altered in *axr3/iaa17* in particular but also in other *arf* or *iaa* mutants (Overvoorde et al., 2005). Consistent with this possibility, expression of *EXPα1* and *XTR8* genes was drastically reduced in response to both ABA and auxin during embryonic axis elongation (see Supplemental Figure 8 online).

Finally, given the variety of the developmental processes regulated by ABA during the seed-to-seedling transition, we sought to identify additional auxin signaling components that could mediate ABA-dependent responses. Together with available whole-genome expression data sets, we found that *AUX1*, *PIN2*, *PIN3*, and *PIN7*, as well as genes encoding auxin-signaling factors, are expressed during germination and subsequent growth. We also found that the high auxin levels in dry seeds are maintained up to 24 h after imbibition. Moreover, *ProIAA2:GUS* and *DR5:GUS* auxin response reporters are active in the vascular tissues of the whole embryo, as well as in the micropylar area, prior to endosperm rupture (see Supplemental Figure 9 online). Endosperm rupture is thought to occur at the micropyle through the combined action of endosperm weakening and pressure from the elongating embryonic axis (Müller et al., 2006). Therefore, it is plausible that ABA-dependent repression of endosperm rupture is also mediated through auxin-dependent regulation of genes encoding cell wall modification enzymes in the micropylar endosperm. Together, these observations indicate that auxin-dependent pathways are operative very early upon seed imbibition.

METHODS

Plant Material

Throughout this study, we used nondormant *Arabidopsis thaliana* seeds without a seed stratification procedure. We refer to seeds imbibed under "normal conditions" when seeds are sown in a standard MS medium containing 0.8% (w/v) agar-agar (VWR).

The *aux1* alleles used in this study (*aux1-7*, *aux1-21*, and *aux1-22* in Col ecotype) were described previously (Bennett et al., 1996) and provided by Cris Kuhlemeier. The *ProAUX1:AUX1-YFP* line (in Col ecotype) used corresponds to the AUX1-YFP116 construct described by Swarup et al. (2004) and was provided by Thierry Gaude. The wild-type and *aux1-100* lines (in Wassilewskija ecotype) expressing the *ProIAA2:GUS* transgene were described by Swarup et al. (2001) and provided by Ranjan Swarup and Malcolm Bennett. The *DR5:GUS* reporter line (in Col ecotype) was initially described by Ulmasov et al. (1997) and provided by Thierry

Gaude. The *pin2* mutant used in this study is the *eir1-1* allele in Col (Roman et al., 1995). The *ProPIN2:PIN2-GFP* line is also in the *eir1-1* background (Xu and Scheres, 2005). Both were provided by Thierry Gaude. *ProPIN3:GUS*, *ProPIN4:GUS*, and *ProPIN7:GUS* transgenic lines in wild-type Col background (Friml et al., 2002a, 2002b, 2003) were obtained from the Nottingham Arabidopsis Stock Centre (NASC; http://Arabidopsis.info/). *pin3-5*, *pin4-3*, and *pin7-2* mutants in Col background (Friml et al., 2002a, 2002b, 2003) were also obtained from the NASC. All *axr2/iaa7* mutants were provided by Jason Reed. *axr2-1* (in Col ecotype) and *axr2-5* (in Wassilewskija ecotype) were previously described (Nagpal et al., 2000). *SALK_089809* insertion line in *AXR2/IAA7* (Col ecotype) is referenced in the SALK SIGnAL database (http://signal.salk.edu/; Alonso et al., 2003). *axr3-1* mutant (Rouse et al., 1998; Nagpal et al., 2000) was provided by Ranjan Swarup. *axr4-2* mutant, described by Dharmasiri et al. (2006), was provided by Lawrence Hobbie. *ProAXR2/IAA7:GUS* (Tian et al., 2002) and *ProAXR3/IAA17:GUS* (Tanimoto et al., 2007) transgenic lines were obtained from Jason Reed and Ottoline Leyser, respectively. *abi3-9* mutant, described by Nambara et al. (2002), was provided by Eiji Nambara. *abi4-1* (Finkelstein et al., 1998) and *abi5-3* (Finkelstein and Lynch, 2000) alleles were provided by Ruth Finkelstein. Other mutants analyzed are listed in Supplemental Table 1 online.

Isolation and Molecular Cloning of *aux1-301/lrt*

A population of 20,000 *abi5-4/Pro35S:ABI5* seeds (M0) was chemically mutagenized using 0.3% ethyl methanesulfonate (64292; Sigma-Aldrich) according to standard procedures (Lightner and Caspar, 1998). The progeny of 15,000 mutagenized seeds was harvested in 15 pools of ~1,000,000 seeds and used to screen for mutant seeds displaying resistance to ABA (0.5 μM) at the level of testa and endosperm rupture as well as embryonic axis elongation, cotyledon expansion, and greening. This led us to identify in five pools three mutants displaying resistance to ABA during germination and early seedling growth. This work focuses on the particular recessive *aux1-301/lrt* locus (see Supplemental Figure 1A online). Map-based cloning was performed as described previously for the *abi5* mutant (Lopez-Molina and Chua, 2000).

Germination and Early Growth Assays

All seed batches compared in this study were harvested on the same day from plants grown side by side (i.e., identical environmental conditions). Dry siliques were obtained ~8 weeks after planting and left for a further 4 weeks at room temperature prior to seed harvesting. Seeds were then permanently stored at 4°C. Seeds obtained in this manner lacked dormancy.

For germination and embryonic axis elongation assays, seeds were surface sterilized by incubation for 10 to 15 min in 70% ethanol and 0.05% SDS and then rinsed in 95% ethanol for 1 min. After drying, they were immediately sown in plates with MS medium containing 0.8% (w/v) agar-agar (20768292; VWR) and 0.5 $g \cdot L^{-1}$ MES. Medium was supplemented with ABA (A1049; Sigma-Aldrich), NAA (N0640; Sigma-Aldrich), 2,4-D (45415; Sigma-Aldrich), NOA (255416; Sigma-Aldrich), BH-IAA, or PEO-IAA (both provided by K. Hayashi) according to the germination condition examined. Plates were incubated in a climate-controlled room (20 to 25°C, 16 h light/day, 70% humidity). Germinating seeds were examined with a Stemi 2000 (Zeiss) stereomicroscope and photographed with a high-resolution digital camera (Canon Power G6, 7.1 megapixels) at different times after seed imbibition, as indicated in the figures. Photographs were analyzed and quantified using the public domain image analysis program ImageJ version 1.38x (http://rsb.info.nih.gov/ij/). For axis elongation rate, we measured the elongation of individual embryonic axes between two time points and took the average of the resulting speed ($n \geq 13$ for all experiments). Error bars in histograms report the SD. We used Student's *t* test (two-tailed assuming unequal variance) to compare average mean values to determine if their differences were statistically significant ($P < 0.01$).

Fluorescence Microscopy

The images were collected using a TCS SP2 AOBS confocal laser microscope (Leica) in the NCCR Frontiers in Genetics bioimaging service (http://www.frontiers-in-genetics.org/).

Measurement and Histochemical Localization of GUS Activity

For measurement of GUS activity, germinating seeds were homogenized by grinding in a mortar and weighed out into Eppendorf tubes. GUS activity was scored by fluorometric measurement using 4-methylumbelliferyl β-D-glucuronide (Sigma-Aldrich) as substrate (Jefferson, 1987). Fluorescence was measured using a TKO 100 minifluorometer (Hoefer Scientific). For histochemical localization, material was fixed in 80% acetone at −20°C for more than 24 h. After rinsing, staining was performed using 5-bromo-4-chloro-3-indoxyl-β-D-glucuronic acid (Biosynth) as substrate (Jefferson, 1987). Reactions were conducted at 37°C in the dark for 15 min to 48 h. Images were collected using a SMZ1500 stereomicroscope (Nikon) coupled to a DS-Fi1 digital camera (Nikon).

RNA Extraction and RNA Gel Blots

Total RNA was extracted as previously described (Vicient and Delseny, 1999). RNA concentrations were measured using a GeneQuant Pro spectrophotometer (Biochrom). RNA gel blot hybridizations were performed by standard procedures; RNA immobilized on membranes was stained with methylene blue and used as a loading control (Sambrook et al., 1989). *AUX1* full-length open reading frame DNA probe was amplified from cDNA with 5′-CACTTAGTTACTAAACACAATCG-3′ and 5′-TGTAAAAAGTACACTATTTTCGTG-3′. *AXR2/IAA7* 3′ untranslated region-specific probe was amplified from cDNA with 5′-GAGAGCAATGGAGAAGTACTG-3′ and 5′-AATAGTAAACATAACAACG-3′. *AXR3/IAA17* 3′ untranslated region-specific probe was amplified from cDNA with 5′-AGTCAAATTAAAAGGATAAGT-3′ and 5′-ATACATAGGAATAGGATGT-3′. *IAA2*-specific probe was amplified from genomic DNA with 5′-ACCAGCTCACCAAGAACA-3′ and 5′-AGCTTCTCTGAGATTCTTCTTCATCACGA-3′. *EXPα1*-specific probe was amplified with 5′-AACTCTTACCTTAACGGA-3′ and 5′-ATAACAAACAAATCTCCA-3′. *XTR8*-specific probe was amplified with 5′-AGTAACCACTCAAAAGGT-3′ and 5′-AGGGTCAAACCACAAGGT-3′. *GH3.5*-specific probe was amplified from genomic DNA with 5′-AGCCCTAACGAGACCATCCT-3′ and 5′-AAGCCATGGATGGTATGAGC-3′. *GH3.6*-specific probe was amplified from cDNA with 5′-CAAAGGCAAAGGGATGTATT-3′ and 5′-GCTCCCAGAATAAGACATAG-3′. *SAUR9*-specific probe was amplified from genomic DNA with 5′-TCCAACTAGCCGAGGAAGA-3′ and 5′-AGCTATTCCTCTCAAGAACCA-3′. Probes were radiolabeled according to standard procedures, and membranes were exposed to phosphorimager screens for quantifications using a Molecular Imager FX scanner (Bio-Rad).

Protein Extraction and Protein Gel Blot

For analysis of HA-ABI5 protein level in the *lrt* mutant, plant protein extracts were resolved under reducing conditions using 10% SDS/polyacrylamide gels. Protein blot was performed as described by Piskurewicz et al. (2008), using the monoclonal HA-probe (F-7) from mouse (Santa Cruz Biotechnology; sc-7392 HRP 200 $\mu g \cdot mL^{-1}$) as a horseradish peroxidase–conjugated primary antibody (diluted 1:10,000).

IAA Level Quantification

Sample Preparation

Material was homogenized (same material as above for measurement of GUS activity) and weighed out into Eppendorf tubes. A cold solution of 0.05 M phosphate buffer, pH 7.0, containing 0.02% DEDTCA was used

for extraction of material. To check the recovery during purification and to validate the quantification, labeled internal standard of $13C_6$-IAA was added to each sample. Samples were stirred for 15 min at 4°C. After centrifugation (5 min, 12,000 rpm, 4°C), supernatant was collected and acidified to pH 2.7 with 1 M HCl. Finally, samples were purified by solid phase extraction on Varian BondElut C_8 (500 mg/3mL) columns, evaporated to dryness, and stored at −20°C before liquid chromatography–mass spectrometry analysis.

Instrumentation

An Acquity UPLC system (Waters), including a binary solvent manager, sample manager, and a Micromass Quattro *micro* API detector (Waters MS Technologies), was used for auxin analysis. All data were processed by MassLynx software with QuanLynx and QuantOptimize programs (version 4.0; Waters).

HPLC-Electrospray Ionization(+)-Tandem Mass Spectrometry Conditions for Sample Analysis

Samples were dissolved in 30 μL of ACN/water (10/90) and filtered (Micro-spin filter tube; 0.2 μm; 3 min at 5700*g*; Grace) and 15 μL of sample was injected onto a reversed-phase column (BetaMax Neutral; 150 × 1 mm; particle size 5 μm; Thermo Scientific) with UNIGUARD column protection (Hypurity advance; 10 × 1 mm; 5 μm; Thermo Scientific). The samples were eluted with a 20-min gradient as follows: 0 to 5 min 90/10 A/B, 5 to 10 min 80/20 A/B, 10 to 18 min 70/30 A/B, 18 to 19 min 50/50 A/B, 19 to 20 10/90 A/B (v/v), where A was 1% ACN with 0.1% formic acid and B was 95% ACN with 0.1% formic acid. At the end of the gradient, the column was equilibrated to initial conditions for 5 min. Flow rate was 0.05 mL min^{-1}, and column was eluted at ambient temperature. Under these conditions, retention time for the monitored IAA was 15.36 min. The effluent was passed to the tandem mass spectrometer without postcolumn splitting. Compounds were quantified by multiple reaction monitoring of $[M+H]^+$ and the appropriate product ions.

For selective multiple reaction monitoring experiments, optimized conditions were as follows: capillary voltage, 3.0 kV; source/desolvation gas temperature, 100/250°C; cone/desolvation gas flow rates, 2.0/450 liters h^{-1}; low-mass and high-mass resolution, 10.0; ion energy 1, 1.0 V; ion energy 2, 1.4 V; multiplier voltages, 700 eV. Argon was used as the collision gas with an optimized pressure of 5×10^{-3} mbar.

The dwell time (IAA = 0.80 s), cone voltages (20 V), and collision energy (15 eV) for diagnostic transitions were optimized to maximize sensitivity.

Calibration curves were created by plotting the known concentration of unlabeled/labeled analyte ratio against the calculated response area of the analyte/internal standard ratio. Limit of detection (IAA = 9.3 fmol) and quantification (IAA = 30.8 fmol) were calculated from signal-to-noise ratios of 3:1 and 10:1, respectively.

Accession Numbers

Sequence data from this article can be found in the Arabidopsis Genome Initiative database under the following accession numbers: *AUX1* (At2g38120), *PIN2* (At5g57090), *PIN3* (At1g70940), *PIN4* (At2g01420), *PIN7* (At1g23080), *AXR2/IAA7* (At3g23050), *AXR3/IAA17* (At1g04250), *IAA2* (At3g23030), *AXR4* (At1g54990), *ABI3* (At3g24650), *ABI4* (At2g40220), *ABI5* (At2g36270), *GH3.5* (At4g27260), *GH3.6* (At5g54510), *SAUR9* (At4g36110), *XTR8* (At3g44990), and *EXPα1* (At1g69530).

Supplemental Data

The following materials are available in the online version of this article.

Supplemental Figure 1. Isolation and Positional Cloning of *long root*, a Previously Undiscovered ABA-Insensitive Locus.

Supplemental Figure 2. *aux1* Is Not Affected in Testa and Endosperm Responses to ABA.

Supplemental Figure 3. ABA Does Not Alter AUX1 Localization and Maintains Low Levels of *AUX1* mRNA Expression.

Supplemental Figure 4. *PIN3*, *PIN4*, and *PIN7* Do Not Participate in the ABA-Dependent Repression of Embryonic Axis Elongation.

Supplemental Figure 5. *AXR2/IAA7* and *AXR3/IAA17* Upstream Sequences Are Transcriptionally Inactive in the Peripheral Elongation Zone in the Presence of ABA.

Supplemental Figure 6. Repression of *axr4* Embryonic Axis Elongation in Response to ABA Is Similar to That of the Wild-Type.

Supplemental Figure 7. ABA Transiently Induces the Expression of Some Auxin-Responsive Genes.

Supplemental Figure 8. Genes Encoding Cell Wall Proteins Are Repressed by Both ABA and Auxin.

Supplemental Figure 9. Auxin Responses Are Active during Germination.

Supplemental Table 1. List of Mutant and Transgenic Lines Used in This Study.

ACKNOWLEDGMENTS

We are especially grateful to Pierre Vassalli for help and numerous suggestions in the writing of this manuscript. We thank Malcolm Bennett and Ranjan Swarup for helpful discussions. We are greatly indebted to the following colleagues for their generous gifts (as detailed in Methods and Supplemental Table 1 online): Ken-ichiro Hayashi, Ranjan Swarup, Malcolm Bennett, Mark Estelle, Jason Reed, Ottoline Leyser, Hiro Nonogaki, Ruth Finkelstein, Cris Kuhlemeier, Lawrence Hobbie, Thierry Gaude, and Xiao-Ya Chen. We thank Christophe Bauer and Jérôme Bosset from the NCCR Frontiers in Genetics Bioimaging service for their help with confocal microscopy. We thank Natsuko Kinoshita, Richard Chappuis, Sandra Oesch, and Yéred Péronnet for their technical support. We wish to thank one reviewer for his helpful clarifications regarding the proper use of certain terms in this manuscript as well as another reviewer for suggesting performing the experiments shown in Figures 5C and 7A. This work was supported by grants from the Swiss National Science Foundation and by the State of Geneva.

Received April 8, 2009; revised July 14, 2009; accepted July 25, 2009; published August 7, 2009.

REFERENCES

Abel, S., Nguyen, M.D., and Theologis, A. (1995). The *PS-IAA4/5*-like family of early auxin-inducible mRNAs in *Arabidopsis thaliana.* J. Mol. Biol. **251:** 533–549.

Alonso, J.M., et al. (2003). Genome-wide insertional mutagenesis of *Arabidopsis thaliana.* Science **301:** 653–657.

Beaudoin, N., Serizet, C., Gosti, F., and Giraudat, J. (2000). Interactions between abscisic acid and ethylene signaling cascades. Plant Cell **12:** 1103–1115.

Benjamins, R., and Scheres, B. (2008). Auxin: The looping star in plant development. Annu. Rev. Plant Biol. **59:** 443–465.

Bennett, M.J., Marchant, A., Green, H.G., May, S.T., Ward, S.P., Millner, P.A., Walker, A.R., Schulz, B., and Feldmann, K.A. (1996). Arabidopsis *AUX1* gene: A permease-like regulator of root gravitropism. Science **273:** 948–950.

Bewley, J.D. (1997). Seed germination and dormancy. Plant Cell **9:** 1055–1066.

Brady, S.M., Sarkar, S.F., Bonetta, D., and McCourt, P. (2003). The *ABSCISIC ACID INSENSITIVE 3* (*ABI3*) gene is modulated by farnesylation and is involved in auxin signaling and lateral root development in *Arabidopsis.* Plant J. **34:** 67–75.

Carles, C., Bies-Etheve, N., Aspart, L., Leon-Kloosterziel, K.M., Koornneef, M., Echeverria, M., and Delseny, M. (2002). Regulation of *Arabidopsis thaliana Em* genes: Role of ABI5. Plant J. **30:** 373–383.

Clouse, S.D. (1996). Molecular genetic studies confirm the role of brassinosteroids in plant growth and development. Plant J. **10:** 1–8.

Collett, C.E., Harberd, N.P., and Leyser, O. (2000). Hormonal interactions in the control of Arabidopsis hypocotyl elongation. Plant Physiol. **124:** 553–562.

Debeaujon, I., and Koornneef, M. (2000). Gibberellin requirement for Arabidopsis seed germination is determined both by testa characteristics and embryonic abscisic acid. Plant Physiol. **122:** 415–424.

Delbarre, A., Muller, P., Imhoff, V., and Guern, J. (1996). Comparison of mechanisms controlling uptake and accumulation of 2,4-dichlorophenoxy acetic acid, naphthalene-l-acetic acid, and indole-3-acetic acid in suspension-cultured tobacco cells. Planta **198:** 532–541.

Dharmasiri, S., Swarup, R., Mockaitis, K., Dharmasiri, N., Singh, S. K., Kowalchyk, M., Marchant, A., Mills, S., Sandberg, G., Bennett, M.J., and Estelle, M. (2006). AXR4 is required for localization of the auxin influx facilitator AUX1. Science **312:** 1218–1220.

Finch-Savage, W.E., and Leubner-Metzger, G. (2006). Seed dormancy and the control of germination. New Phytol. **171:** 501–523.

Finkelstein, R.R. (1994). Mutations at two new *Arabidopsis* ABA response loci are similar to the *abi3* mutations. Plant J. **5:** 765–771.

Finkelstein, R.R., Gampala, S.S., and Rock, C.D. (2002). Abscisic acid signaling in seeds and seedlings. Plant Cell **14**(Suppl): S15–S45.

Finkelstein, R.R., and Lynch, T.J. (2000). The *Arabidopsis* abscisic acid response gene *ABI5* encodes a basic leucine zipper transcription factor. Plant Cell **12:** 599–609.

Finkelstein, R.R., Wang, M.L., Lynch, T.J., Rao, S., and Goodman, H. M. (1998). The *Arabidopsis* abscisic acid response locus *ABI4* encodes an APETALA 2 domain protein. Plant Cell **10:** 1043–1054.

Fleming, A.J. (2006). Plant signalling: The inexorable rise of auxin. Trends Cell Biol. **16:** 397–402.

Friml, J., Benkova, E., Blilou, I., Wisniewska, J., Hamann, T., Ljung, K., Woody, S., Sandberg, G., Scheres, B., Jurgens, G., and Palme, K. (2002b). *AtPIN4* mediates sink-driven auxin gradients and root patterning in Arabidopsis. Cell **108:** 661–673.

Friml, J., Vieten, A., Sauer, M., Weijers, D., Schwarz, H., Hamann, T., Offringa, R., and Jurgens, G. (2003). Efflux-dependent auxin gradients establish the apical-basal axis of Arabidopsis. Nature **426:** 147–153.

Friml, J., Wisniewska, J., Benkova, E., Mendgen, K., and Palme, K. (2002a). Lateral relocation of auxin efflux regulator PIN3 mediates tropism in Arabidopsis. Nature **415:** 806–809.

Ghassemian, M., Nambara, E., Cutler, S., Kawaide, H., Kamiya, Y., and McCourt, P. (2000). Regulation of abscisic acid signaling by the ethylene response pathway in *Arabidopsis*. Plant Cell **12:** 1117–1126.

Gray, W.M., Ostin, A., Sandberg, G., Romano, C.P., and Estelle, M. (1998). High temperature promotes auxin-mediated hypocotyl elongation in Arabidopsis. Proc. Natl. Acad. Sci. USA **95:** 7197–7202.

Guilfoyle, T.J., and Hagen, G. (2007). Auxin response factors. Curr. Opin. Plant Biol. **10:** 453–460.

Hayashi, K., Hatate, T., Kepinski, S., and Nozaki, H. (2008a). Design and synthesis of auxin probes specific to TIR1, auxin receptor. Regul. Plant Growth Dev. **43** (suppl.), 95.

Hayashi, K., Tan, X., Zheng, N., Hatate, T., Kimura, Y., Kepinski, S., and Nozaki, H. (2008b). Small-molecule agonists and antagonists of F-box protein-substrate interactions in auxin perception and signaling. Proc. Natl. Acad. Sci. USA **105:** 5632–5637.

Holdsworth, M.J., Bentsink, L., and Soppe, W.J.J. (2008). Molecular networks regulating Arabidopsis seed maturation, after-ripening, dormancy and germination. New Phytol. **179:** 33–54.

Hugouvieux, V., Kwak, J.M., and Schroeder, J.I. (2001). An mRNA cap binding protein, ABH1, modulates early abscisic acid signal transduction in Arabidopsis. Cell **106:** 477–487.

Jefferson, R. (1987). Assaying chimeric genes in plants: The *GUS* gene fusion system. Plant Mol. Biol. Rep. **5:** 387–405.

Jenik, P.D., Gillmor, C.S., and Lukowitz, W. (2007). Embryonic patterning in *Arabidopsis thaliana.* Annu. Rev. Cell Dev. Biol. **23:** 207–236.

Kerr, I.D., and Bennett, M.J. (2007). New insight into the biochemical mechanisms regulating auxin transport in plants. Biochem. J. **401:** 613–622.

Knox, K., Grierson, C.S., and Leyser, O. (2003). *AXR3* and *SHY2* interact to regulate root hair development. Development **130:** 5769–5777.

Koornneef, M., Reuling, G., and Karssen, C.M. (1984). The isolation and characterization of abscisic acid-insensitive mutants of *Arabidopsis thaliana.* Physiol. Plant. **61:** 377–383.

Kramer, E.M., and Bennett, M.J. (2006). Auxin transport: A field in flux. Trends Plant Sci. **11:** 382–386.

Kucera, B., Cohn, M.A., and Leubner-Metzger, G. (2005). Plant hormone interactions during seed dormancy release and germination. Seed Sci. Res. **15:** 281–307.

Lightner, J., and Caspar, T. (1998). Seed mutagenesis of Arabidopsis. In Arabidopsis Protocols, J.M. Martinez-Zapater and J. Salinas, eds (Totowa, NJ: Humana Press), pp. 91–103.

Lin, Y., and Schiefelbein, J. (2001). Embryonic control of epidermal cell patterning in the root and hypocotyl of Arabidopsis. Development **128:** 3697–3705.

Liu, P.P., Montgomery, T.A., Fahlgren, N., Kasschau, K.D., Nonogaki, H., and Carrington, J.C. (2007). Repression of *AUXIN RESPONSE FACTOR10* by microRNA160 is critical for seed germination and post-germination stages. Plant J. **52:** 133–146.

Lopez-Molina, L., and Chua, N.H. (2000). A null mutation in a bZIP factor confers ABA-insensitivity in *Arabidopsis thaliana.* Plant Cell Physiol. **41:** 541–547.

Lopez-Molina, L., Mongrand, S., and Chua, N.H. (2001). A postgermination developmental arrest checkpoint is mediated by abscisic acid and requires the ABI5 transcription factor in *Arabidopsis.* Proc. Natl. Acad. Sci. USA **98:** 4782–4787.

Lopez-Molina, L., Mongrand, S., McLachlin, D.T., Chait, B.T., and Chua, N.H. (2002). ABI5 acts downstream of ABI3 to execute an ABA-dependent growth arrest during germination. Plant J. **32:** 317–328.

Marchant, A., Kargul, J., May, S.T., Muller, P., Delbarre, A., Perrot-Rechenmann, C., and Bennett, M.J. (1999). AUX1 regulates root gravitropism in *Arabidopsis* by facilitating auxin uptake within root apical tissues. EMBO J. **18:** 2066–2073.

Müller, A., Guan, C., Gälweiler, L., Tanzler, P., Huijser, P., Marchant, A., Parry, G., Bennett, M., Wisman, E., and Palme, K. (1998). *AtPIN2* defines a locus of *Arabidopsis* for root gravitropism control. EMBO J. **17:** 6903–6911.

Müller, K., Tintelnot, S., and Leubner-Metzger, G. (2006). Endosperm-limited Brassicaceae seed germination: Abscisic acid inhibits embryo-induced endosperm weakening of *Lepidium sativum* (cress) and endosperm rupture of cress and *Arabidopsis thaliana.* Plant Cell Physiol. **47:** 864–877.

Muto, H., Watahiki, M.K., Nakamoto, D., Kinjo, M., and Yamamoto, K.T. (2007). Specificity and similarity of functions of the *Aux/IAA* genes in auxin signaling of Arabidopsis revealed by promoter-exchange experiments among *MSG2/IAA19, AXR2/IAA7*, and *SLR/IAA14.* Plant Physiol. **144:** 187–196.

Nagpal, P., Walker, L.M., Young, J.C., Sonawala, A., Timpte, C., Estelle, M., and Reed, J.W. (2000). *AXR2* encodes a member of the Aux/IAA protein family. Plant Physiol. **123:** 563–574.

Nakabayashi, K., Okamoto, M., Koshiba, T., Kamiya, Y., and Nambara, E. (2005). Genome-wide profiling of stored mRNA in *Arabidopsis thaliana* seed germination: epigenetic and genetic regulation of transcription in seed. Plant J. **41:** 697–709.

Nambara, E., and Marion-Poll, A. (2005). Abscisic acid biosynthesis and catabolism. Annu. Rev. Plant Biol. **56:** 165–185.

Nambara, E., Suzuki, M., Abrams, S., McCarty, D.R., Kamiya, Y., and McCourt, P. (2002). A screen for genes that function in abscisic acid signaling in *Arabidopsis thaliana.* Genetics **161:** 1247–1255.

Nawy, T., Lukowitz, W., and Bayer, M. (2008). Talk global, act local-patterning the *Arabidopsis* embryo. Curr. Opin. Plant Biol. **11:** 28–33.

Ni, D.A., Wang, L.J., Ding, C.H., and Xu, Z.H. (2001). Auxin distribution and transport during embryogenesis and seed germination of Arabidopsis. Cell Res. **11:** 273–278.

Ogawa, M., Hanada, A., Yamauchi, Y., Kuwahara, A., Kamiya, Y., and Yamaguchi, S. (2003). Gibberellin biosynthesis and response during Arabidopsis seed germination. Plant Cell **15:** 1591–1604.

Olszewski, N., Sun, T.P., and Gubler, F. (2002). Gibberellin signaling: Biosynthesis, catabolism, and response pathways. Plant Cell **14** (suppl.): S61–S80.

Overvoorde, P.J., et al. (2005). Functional genomic analysis of the *AUXIN/INDOLE-3-ACETIC ACID* gene family members in *Arabidopsis thaliana.* Plant Cell **17:** 3282–3300.

Parcy, F., Valon, C., Raynal, M., Gaubier-Comella, P., Delseny, M., and Giraudat, J. (1994). Regulation of gene expression programs during *Arabidopsis* seed development: roles of the *ABI3* locus and of endogenous abscisic acid. Plant Cell **6:** 1567–1582.

Parry, G., Delbarre, A., Marchant, A., Swarup, R., Napier, R., Perrot-Rechenmann, C., and Bennett, M.J. (2001). Novel auxin transport inhibitors phenocopy the auxin influx carrier mutation *aux1.* Plant J. **25:** 399–406.

Penfield, S., Li, Y., Gilday, A.D., Graham, S., and Graham, I.A. (2006). *Arabidopsis* ABA INSENSITIVE4 regulates lipid mobilization in the embryo and reveals repression of seed germination by the endosperm. Plant Cell **18:** 1887–1899.

Piskurewicz, U., Jikumaru, Y., Kinoshita, N., Nambara, E., Kamiya, Y., and Lopez-Molina, L. (2008). The gibberellic acid signaling repressor RGL2 inhibits *Arabidopsis* seed germination by stimulating abscisic acid synthesis and ABI5 activity. Plant Cell **20:** 2729–2745.

Piskurewicz, U., Tureckova, V., Lacombe, E., and Lopez-Molina, L. (2009). Far-red light inhibits germination through DELLA-dependent stimulation of ABA synthesis and ABI3 activity. EMBO J. **28:** 2259–2271.

Quint, M., and Gray, W.M. (2006). Auxin signaling. Curr. Opin. Plant Biol. **9:** 448–453.

Riefler, M., Novak, O., Strnad, M., and Schmulling, T. (2006). *Arabidopsis* cytokinin receptor mutants reveal functions in shoot growth, leaf senescence, seed size, germination, root development, and cytokinin metabolism. Plant Cell **18:** 40–54.

Rock, C.D., and Sun, X. (2005). Crosstalk between ABA and auxin signaling pathways in roots of *Arabidopsis thaliana* (L.) Heynh. Planta **222:** 98–106.

Roman, G., Lubarsky, B., Kieber, J.J., Rothenberg, M., and Ecker, J.R. (1995). Genetic analysis of ethylene signal transduction in *Arabidopsis thaliana*: Five novel mutant loci integrated into a stress response pathway. Genetics **139:** 1393–1409.

Romano, C.P., Robson, P.R., Smith, H., Estelle, M., and Klee, H. (1995). Transgene-mediated auxin overproduction in Arabidopsis: Hypocotyl elongation phenotype and interactions with the *hy6-1* hypocotyl elongation and *axr1* auxin-resistant mutants. Plant Mol. Biol. **27:** 1071–1083.

Rouse, D., Mackay, P., Stirnberg, P., Estelle, M., and Leyser, O. (1998). Changes in auxin response from mutations in an *AUX/IAA* gene. Science **279:** 1371–1373.

Sambrook, J., Fritsch, E.F., and Maniatis, T. (1989). Molecular Cloning: A Laboratory Manual. (Cold Spring Harbor, NY: Cold Spring Harbor Laboratory Press).

Scheres, B., Wolkenfelt, H., Willemsen, V., Terlouw, M., Lawson, E., Dean, C., and Weisbeek, P. (1994). Embryonic origin of the Arabidopsis primary root and root meristem initials. Development **120:** 2475–2487.

Smalle, J., Haegman, M., Kurepa, J., Van Montagu, M., and Straeten, D.V. (1997). Ethylene can stimulate *Arabidopsis* hypocotyl elongation in the light. Proc. Natl. Acad. Sci. USA **94:** 2756–2761.

Steber, C.M., and McCourt, P. (2001). A role for brassinosteroids in germination in Arabidopsis. Plant Physiol. **125:** 763–769.

Swarup, R., Friml, J., Marchant, A., Ljung, K., Sandberg, G., Palme, K., and Bennett, M. (2001). Localization of the auxin permease AUX1 suggests two functionally distinct hormone transport pathways operate in the *Arabidopsis* root apex. Genes Dev. **15:** 2648–2653.

Swarup, R., et al. (2004). Structure-function analysis of the presumptive *Arabidopsis* auxin permease AUX1. Plant Cell **16:** 3069–3083.

Tanimoto, M., Jowett, J., Stirnberg, P., Rouse, D., and Leyser, O. (2007). *pax1-1* partially suppresses gain-of-function mutations in *Arabidopsis AXR3/IAA17.* BMC Plant Biol. **7:** 20.

Teale, W.D., Paponov, I.A., and Palme, K. (2006). Auxin in action: Signalling, transport and the control of plant growth and development. Nat. Rev. Mol. Cell Biol. **7:** 847–859.

Tian, Q., Uhlir, N.J., and Reed, J.W. (2002). Arabidopsis SHY2/IAA3 inhibits auxin-regulated gene expression. Plant Cell **14:** 301–319.

Timpte, C., Wilson, A.K., and Estelle, M. (1994). The *axr2-1* mutation of *Arabidopsis thaliana* is a gain-of-function mutation that disrupts an early step in auxin response. Genetics **138:** 1239–1249.

Ulmasov, T., Murfett, J., Hagen, G., and Guilfoyle, T.J. (1997). Aux/IAA proteins repress expression of reporter genes containing natural and highly active synthetic auxin response elements. Plant Cell **9:** 1963–1971.

Vicient, C.M., and Delseny, M. (1999). Isolation of total RNA from *Arabidopsis thaliana* seeds. Anal. Biochem. **268:** 412–413.

Wang, J.W., Wang, L.J., Mao, Y.B., Cai, W.J., Xue, H.W., and Chen, X.Y. (2005). Control of root cap formation by microRNA-targeted auxin response factors in *Arabidopsis*. Plant Cell **17:** 2204–2216.

Weijers, D., Benkova, E., Jager, K.E., Schlereth, A., Hamann, T., Kientz, M., Wilmoth, J.C., Reed, J.W., and Jurgens, G. (2005). Developmental specificity of auxin response by pairs of ARF and Aux/IAA transcriptional regulators. EMBO J. **24:** 1874–1885.

Wilson, A.K., Pickett, F.B., Turner, J.C., and Estelle, M. (1990). A dominant mutation in *Arabidopsis* confers resistance to auxin, ethylene and abscisic acid. Mol. Gen. Genet. **222:** 377–383.

Winter, D., Vinegar, B., Nahal, H., Ammar, R., Wilson, G.V., and Provart, N.J. (2007). An "electronic fluorescent pictograph" browser for exploring and analyzing large-scale biological data sets. PLoS ONE **2:** e718.

Xu, J., and Scheres, B. (2005). Dissection of *Arabidopsis* ADP-RIBOSYLATION FACTOR 1 function in epidermal cell polarity. Plant Cell **17:** 525–536.

Yang, Y., Hammes, U.Z., Taylor, C.G., Schachtman, D.P., and Nielsen, E. (2006). High-affinity auxin transport by the AUX1 influx carrier protein. Curr. Biol. **16:** 1123–1127.